Functional Characterization of Protein PDIA3

Doctor of Philosophy in Biochemistry

XXXI Cycle (2015-2018)

Department of Biochemical Sciences
"Alessandro Rossi Fanelli"

Candidate
Flavia Giamogante

Thesis Advisor
Prof. F. Altieri

PhD Cordinator
Prof. S. Gianni

A papa',
alla mia terra e
alla sua gente…

Table of Contents

Introduction

1.1. Protein Disulfide Isomerase family: a member of the thioredoxin superfamily

Thioredoxins (Trx) are small globular proteins that are found in all living cells from archeabacteria to humans [Holmgren, 1985]. The 3-D structures of Trx proteins are highly conserved and are characterized by a central core, consisting of five β-sheets surrounded by four α-helices and their active sites are characterized by the CXXC sequence, also known as the "Trx-motif" (Fig. 1) [Holmgren, 1995; Martin et al., 1995]. This structural configuration is known as thioredoxin fold and is present in different protein families, such as protein disulfide isomerases (PDIs), in DSB (disulphide bond formation) proteins, in glutaredoxin (Grx), in the glutathione reductase and glutathione peroxidase. The structural features that are conserved in Trx family members, such as the Trx-fold and the specific primary and secondary structures, lead to a different reactivity in catalyzing protein disulfide interchange reactions. It has been shown that both active site cysteine residues play an important role in the differentiation of the properties across the family and the relative stability (depending on cysteines nucleophilicity) of thiolates determines whether these enzymes catalyze oxidation, reduction or isomerization of thiol

residues in protein substrates [Cheng et al., 2011; Hatahet et al., 2009; Carvalho et al., 2009].

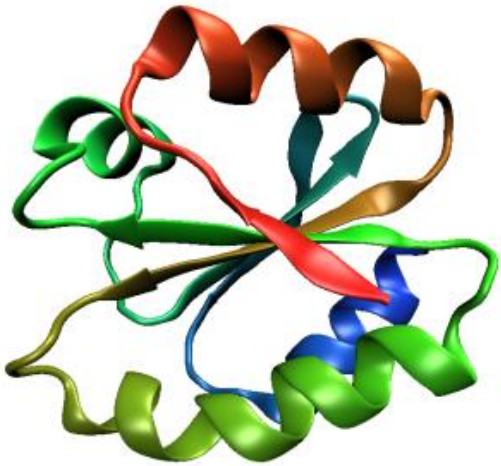

Figure 1. The typical Trx-fold.

PDI proteins with active Trx-domains are generally localized in the lumen of the endoplasmic reticulum (ER), where they mediate thiol-disulfide interchanges critical during post-translational protein folding [Galligan & Petersen, 2012].

The protein disulfide isomerase (PDI) family is composed of 21 known proteins in humans, that belong to the thioredoxin superfamily, classified by sequence and structural homology (Fig. 2).

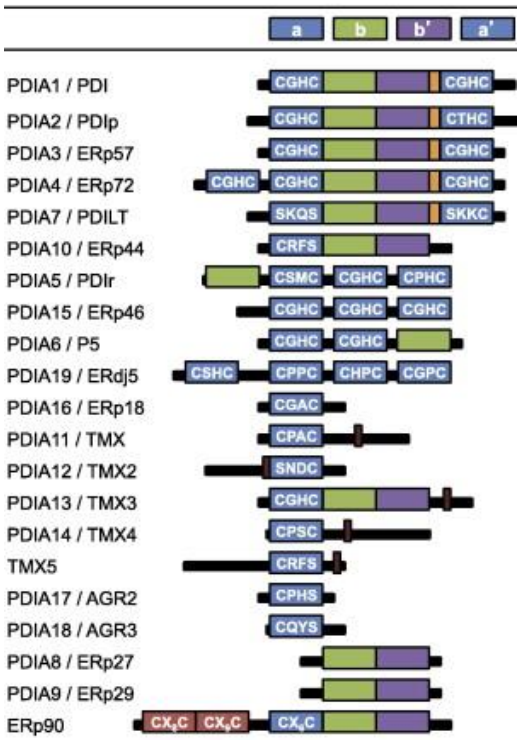

Figure 2. PDI family members in humans. In blue: catalytic domains a and a', in green and purple non-catalytic b and b' domains.

These enzymes catalyze the formation, reduction or isomerization of disulfide bonds of newly synthesized proteins in the lumen of the endoplasmic reticulum (ER). They are also part of a quality-control system, thanks to their molecular chaperone function. These proteins show a structural organization with multiple domains; each domain shows the typical Trx-fold and two or three of these domains contain the redox-active -CXXC- motif, while the others are considered Trx inactive domains [Turano et al., 2002]. Because of these redox-inactive domains, PDIs have the ability to bind peptides or proteins and to exert a molecular chaperone function [Ferrari et al., 1999; Ellgaard et al., 2005]. The number, the arrangement of tioredoxin-like domains and the specific sequence of the catalytic -CXXC-

motif can be used to differentiate the members of this family. These differences determine their distinct role in the oxidative folding, but also contribute to their specific functions in other pathways. Furthermore, the differences in their redox active motifs can reflect separated roles in oxidation, reduction and isomerization (Fig. 3) [Kozlov et al., 2006].

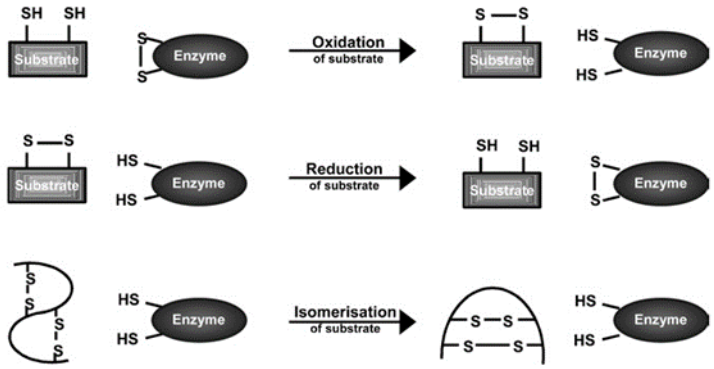

Figure 3. PDIs disulphide bond exchange. Depending on the redox form, they can catalyse oxidation, reduction or isomerization.

1.2. PDIA3 protein

1.2.1. PDIA3 structure and functions

PDIA3, also known as ERp57, ERp60, GRP58, and 1,25D3-MARRS; encoded by *PDIA3*, is a prominent member of the PDI family that has attracted significant attention by the research community. PDIA3 was first detected as a stress-responsive protein with upregulated expression following glucose depletion-induced cellular stress [Lee et al., 1981]. Trx-like domains of the PDI proteins are present as catalytically active domains (a or a′) or

inactive domains (b or b′). Each domain contains a Trx-like fold with alternating α-helices and β-strands [Ferrari et al., 1999; Kozlov et al., 2006; Silvennoinen et al., 2004]. PDIA3 is structurally similar to PDI, containing four TRX-like domains (a-b-b′-a′; Fig. 4), with matching redox active CGHC motifs and similar reduction potentials of the enzymes dual catalytic domains [Hatahet & Ruddock, 2009; Kozlov et al., 2006].

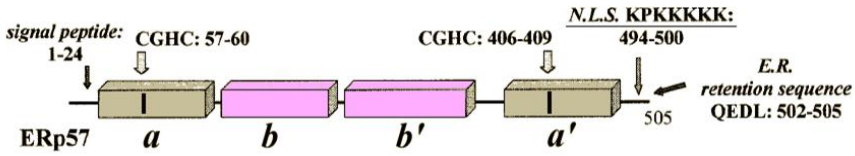

Figure 4. PDIA3 Protein modular structure.

The catalytically inactive central domains, b and b′, have a vital role in the specific functionality of PDIA3 in protein binding and folding. The N-terminal signal sequence directs initial ER localization while the C-terminus contains a QDEL ER retention/retrieval motif [Khanal & Nemere, 2007]. PDIA3 is classically considered an ER resident protein, but also contains a nuclear location sequence. Indeed, there are evidences that the stimulation with various macrophage differentiation-inducing agents and cellular stressors is able to induce PDIA3 transfer from cytoplasm to nucleus [Grillo et al., 2006; Grindel et al., 2011; Wu et al., 2010]. PDIA3 has also been detected on cell surface [Khanal & Nemere, 2007], as well as in mitochondria [He et al., 2014; Ozaki et al., 2008]. Regardless of the mechanism(s) underlying PDIA3's subcellular localization, it is clear that the enzyme's activity is not limited to those attributed to classical ER-resident proteins (Fig. 5).

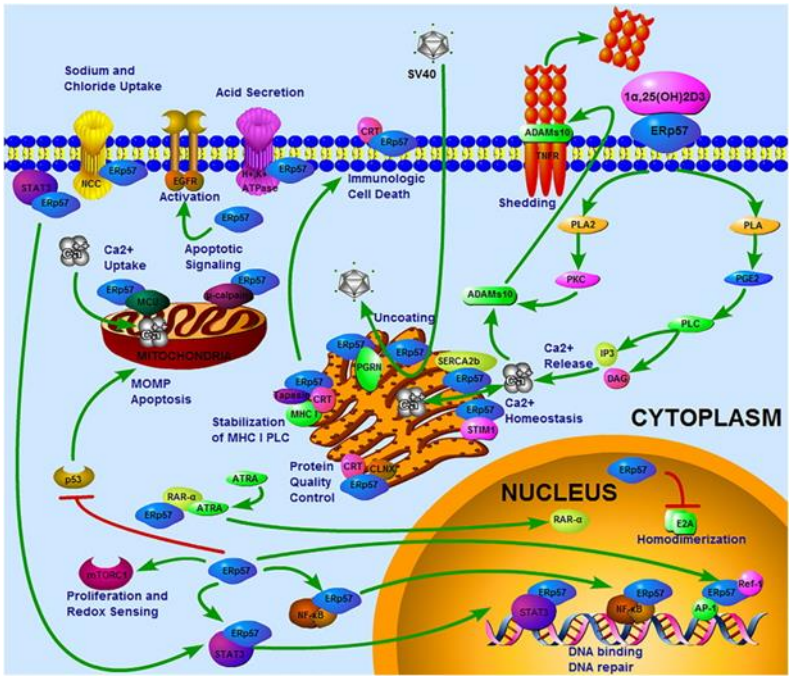

Figure 5. Representative PDIA3 cellular localizations and functions.

1.2.2. PDIA3 localization in the ER

PDIA3 is mainly located in the ER, where it participates to the correct folding and to the quality control of neo-synthesized glycoproteins destined to be secreted or localized to the cell membrane. To do this, PDIA3 interacts with lectins calreticulin (CRT) or calnexin (CNX), which are responsible for recognizing and binding to monoglycosylated proteins [Oliver et al., 1997; Molinari et al., 1999; Oliver et al., 1999]. It has been reported that modifications of specific residues in the b' domain of PDIA3 reduce or abolish its binding to calreticulin, indicating that this domain is responsible for this interaction [Russell et al., 2004]. PDIA3, in complex with CRT/CNX, performs disulfide shuffling, a process that requires the intermediate formation of a mixed disulfide between the glycoprotein and the proximal

cysteine of one of the two active sites of PDIA3. The shuffling is then completed by the intervention of the distal cysteine present in the same active site. A second important function of PDIA3 in the ER is the participation in the assembly of the major histocompatibility complex (MHC) class I [Lindquist e al., 1998]. An efficient antigen processing through the MHC I requires the formation of the peptide-loading complex (PLC). This complex consists of the transporter associated with antigen processing (TAP) as centerpiece, which recruits the major histocompatibility complex class I (MHC I) heavy-chain/β2-microglobulin dimer by the adapter protein tapasin (Tsn). The transient Tsn-MHC I interaction is stabilized by PDIA3, and the endoplasmic reticulum (ER) chaperone calreticulin (CRT), which recognizes the monoglucose unit of N-core glycosylated MHC I molecules. In the PLC, PDIA3 interacts with tapasin [Dick et al., 2002]; the structure of this complex has been resolved at 2.6 Å resolution [Dong et al., 2009]; this was the first time in which the whole 3D structure of PDIA3 was obtained. Both a and a' domains of PDIA3 are involved in the interaction with tapasin. The cysteine 57 in the a domain of PDIA3 forms a disulfide bond with cysteine 95 of tapasin, while the a' domain-tapasin interaction is entirely non-covalent. The tapasin-PDIA3 complex is essential in the assembly and the stabilization of the PLC where PDIA3 shows a structural role rather than a catalytic one. In fact, the suppression of PDIA3 affects the stability of PLC and decreases both the expression of MHC I on the cell surface and the peptide loading within the PLC [Garbi et al., 2006]. PDIA3 also modulates the activity of the sarco/endoplasmic reticulum calcium ATPase (SERCA), a Ca^{2+}-ATPase that transfers Ca^{2+} from the cytosol to the lumen of the ER, by regulating the redox state of the sulfhydryl groups in the intraluminal domain of SERCA [Li et al., 2004].

1.2.3. PDIA3 localization in the cytosol

PDIA3 has been reported in the cytosol thanks to its interaction with other proteins. In this localization, it associates with STAT3 [Sehgal, 2003]. STAT3 is a member of the STAT (Signal Transducer and Activator of Transcription) family. In response to cytokines and growth factors, these proteins are phosphorylated by receptor-associated kinases and then form homo- or hetero-dimers that translocate to the cell nucleus, where they act as transcription activators. STAT3 is activated through phosphorylation of tyrosine 705, in response to various cytokines and growth factors including interferons, epidermal growth factor and interleukin-6 (IL-6). The binding of IL-6 family cytokines to gp130 receptor triggers STAT3 phosphorylation by JAK2. Hyperactivation of STAT3 is frequently observed in a variety of human cancers, including head and neck cancer [Yu et al., 2004; Yu et al, 2009; Song et al., 2000]. Continuous STAT3 activation allows the growth and survival of cancer cells through modulation of cell cycle regulators (e.g., cyclin D1/D2 and c-Myc), upregulation of anti-apoptotic proteins (e.g., Mcl-1, Bcl-xl, and survivin), downregulation of the tumor suppressor p53, and induction of angiogenesis by vascular endothelial growth factor (VEGF); these mechanisms lead to tumor progression and resistance to anti-cancer drugs [Frank, 2013; Yu et al., 2004; Yu et al, 2009]. It has been reported that PDIA3 modulates STAT3 activity [Eufemi et al., 2004; Chichiarelli et al., 2010], although there are controversial results [Coe et al., 2010]. For instance, PDIA3 has been reported to interact with STAT3 and enhance its activity in melanoma and hepatoma cells [Eufemi et al., 2004; Chichiarelli et al., 2010], whereas other research suggested that this PDIA3-STAT3 complex negatively affects STAT3 DNA-binding activity [Coe et al., 2010].

Hence, the role of PDIA3 in the STAT3 activity regulation is not completely defined yet.

As a further proof of PDIA3 presence in the cytosol, it was found in association with mTOR [Ramírez-Rangel et al., 2011]. mTOR is a serine-threonine protein kinase, found in two multiprotein complexes called mTORC1 and mTORC2, which regulate cell proliferation. PDIA3 contributes to the assembly of mTORC1, activates the kinase activity of mTOR, and also participates in the mechanism by which mTORC1 detects its upstream signals, such as stimulation by insulin or nutrients. PDIA3 over-expression induces cellular proliferation, while PDIA3 knockdown opposes the proliferation induced by insulin and nutrients. It is reasonable that part of this behavior is related to the mTOR-PDIA3 interaction, considering that mTOR is involved in the regulation of proliferation [Ramírez-Rangel et al., 2011].

1.2.4. PDIA3 localization in the nucleus

PDIA3 was found for the first time in the nuclei of 3T3 cells and rat spermatids [Ohtani et al., 1993] and of chicken hepatocytes, where PDIA3 was found mainly in the internal nuclear matrix fraction [Altieri et al., 1993]. This observation was not easily accepted initially, because it was considered unlikely that a protein provided with an ER retention signal can escape from the endoplasmic reticulum. However, nowadays there is strong experimental evidence, provided by different laboratories with a variety of experimental techniques, that PDIA3 can be found in the nucleus. It has been shown that PDIA3 is present in the nuclei of HeLa cells and that it interacts directly with DNA [Coppari et al., 2002]. PDIA3 interacts preferentially with A/T rich regions, and in general with DNA regions typical of the MARs (nuclear matrix associated regions) [Coppari et al., 2002; Ferraro et al., 1999]. The

DNA fragments immunoprecipitated with an anti-PDIA3 antibody from HeLa and Raji cells were enriched in sequences contained either in introns or in 5'-flanking regions of known genes [Chichiarelli et al., 2007; Chichiarelli et al., 2010]. This can be compatible with a gene expression regulatory function. Furthermore, the consensus sequences for STAT3 were found to be associated both with this transcription factor and with PDIA3 [Chichiarelli et al., 2010]. Because of the relatively low affinity for DNA and its lack of stringent sequence specificity, PDIA3 cannot itself be considered as a transcription factor, but it might be considered an accessory protein for transcription regulation, possibly maintaining the transcription factors in their proper redox state.

Moreover, PDIA3 shows in vitro DNA-binding properties that are strongly dependent on the redox state of the protein. The DNA binds to the a' domain [Grillo et al., 2002] and the binding requires the oxidized form of PDIA3 [Ferraro et al., 1999; Grillo et al, 2007]. Evidences, from M14 melanoma cells and HepG2 hepatoma cells, demonstrated the association of STAT3 and PDIA3 also in the nucleus at the level of DNA interaction [Eufemi et al., 2004; Chichiarelli et al., 2010]. The PDIA3 silencing in M14 cells causes a decrease in the expression of the STAT3-dependent gene CRP [Chichiarelli et al., 2010], suggesting the possibility of a positive involvement of PDIA3 in the signalling and/or DNA binding of STAT3.

In NB4 leukemia cells, PDIA3 and NFkB translocate to the nucleus after treatment with calcitriol and phorbol ester [Wu et al., 2010], hypothesizing, again, a role of PDIA3 in the control of gene expression through regulation of the conformation of associated transcription factors.

Finally, PDIA3 displays in vitro and in vivo affinity for Ref-1, a protein involved in DNA repair as well as in the reduction and activation of transcription factors. These two proteins appear to cooperate in the activation of a variety of transcription factors, which need to be in their reduced form in order to bind DNA [Grillo et al.,2006].

1.2.5. PDIA3 localization on cell membrane

The first time in which it was observed that PDIA3 can escape from the ER was when Hirano and colleagues noticed that the protein was being secreted from 3T3 cells [Hirano et al., 1995]. Afterwards several studies showed that PDIA3 could be found on the cell surface or in complexes with cell membrane proteins.

PDIA3 has been found on the surface of the sperm head, where it is required for sperm-egg fusion [Ellerman et al., 2006]. Possibly the PDIA3 role is related to the thiol-disulfide exchange reactions necessary for the gamete fusion process.

One of the functions of PDIA3 on the cell surface is the binding of the hydroxylated, hormonal form of vitamin D3, i.e., 1α,25-dihydroxycholecalciferol (1α,25-(OH)2D3, calcitriol) [Nemere et al., 2004], followed by activation of non-genomic responses and the internalization and nuclear import of PDIA3 itself.

It has been demonstrated that PDIA3 exists in caveolae, where it interacts with phospholipase A2 (PLA2) activating protein (PLAA) and caveolin-1 to initiate a rapid signaling in musculoskeletal cells via PLA2, phospholipase C (PLC), protein kinase C (PKC) and the ERK1/2 family of mitogen activated protein kinases (MAPK) [Boyan et al., 2012].

Moreover, it was recently reported that PDIA3 is associated and co-localizes with β-DG (one of the two subunit of the extracellular receptor dystroglycan,

DG) at the plasma membrane of 293-Ebna cells. It has been argued that PDIA3 may assist DG during its post-translational maturation or that it could modulate DG redox state [Sciandra et al., 2012].

PDIA3 is also present on the platelet surface and it has been showed that its inhibition blocks platelet activation [Holbrook et al., 2012; Wu et al., 2012]. PDIA3 is secreted by platelets and endothelial cells upon vascular injury and accumulates in the thrombus, where it regulates the activation and recruitment of other platelets [Holbrook et al., 2012].

Dihazi and colleagues [Dihazi et al., 2011] showed that PDIA3 was found to be secreted by renal cells in high amounts upon profibrotic cytokine treatment, and to interact with extracellular matrix (ECM) proteins, such as fibronectin and collagen. These data suggest that secreted PDIA3 could participate in ECM synthesis and stabilization, thus potentially leading to a progressive renal fibrosis.

1.3. PDIA3 and diseases

PDIA3 has been associated with several human diseases such as cancer, prion disorders, Alzheimer's disease, Parkinson's disease and hepatitis [Hetz et al., 2005; Martin et al., 1993; Muhlenkamp and Gill, 1998; Seliger et al., 2001; Erickson et al., 2005; Tourkova et al., 2005]. PDIA3 expression is increased in transformed cells, and it is thought that its role in oncogenic transformation is directly due to its ability to control intracellular and extracellular redox activities [Hirano et al., 1995]. An increase in PDIA3 expression has also been observed in the early stages of prion disease, suggesting that it may play a neuroprotective role in the cellular response to prion infection [Hetz et al., 2005]. Parkinson's disease is characterized by the

progressive loss of dopaminergic neurons of the substantia nigra. It has been shown that the treatment of cell lines with 6-hydroxidopamine (6-OHDA, a Parkinson mimetic neurotoxin that selectively kills dopaminergic neurons) induces PDIA3 oxidation and PDIA3-DNA conjugates formation. It was suggested that PDIA3 plays an early adaptive response in toxin-mediated stress [Kim-Han et al., 2007].

1.3.1. PDIA3 and Alzheimer's disease

Alzheimer's disease (AD) is a progressive, neurodegenerative disorder that is associated clinically with a progressive cognitive impairment [Cummings, 2004]. AD histology is characterized by the accumulation of amyloid β-peptide (Aβ) plaques and neurofibrillary tangles composed of hyperphosphorylated tau protein [Cummings et al., 2004]. The endoplasmic reticulum (ER) stress response is regarded as an important process in the aetiology of AD [see for review Hashimoto and Saido, 2018]. The accumulation of pathogenic misfolded proteins and the disruption of intracellular calcium signalling are considered to be fundamental mechanisms that underlie the induction of ER stress, leading to neuronal cell death. A number of reports have indicated that Aβ oligomers or fibrils trigger ER stress in in vitro experimental systems based on primary cultures of neuronal cells, cell lines and brain slices [Nishitsuji et al., 2009; Alberdi et al., 2013; Seyb et al., 2006]. Further investigations have proposed mechanisms establishing a connection between extracellular Aβ and intracellular ER. The most likely mediator between Aβ and ER stress is calcium, with the binding of Aβ to glutaminergic receptors likely to induce ER stress-dependent cell death by disrupting cytosolic calcium homeostasis [Costa et al., 2012]. In this scenario, a crucial role seems to be play by the mechanisms for promoting the clearance of neurotoxic and/or misfolded proteins, a strategy that may curtail

the onset and slow the progression of AD. Recent studies are exploring the involvement of the PDIA3 in the response to several types of stress in different neurodegenerative diseases, such as AD, Parkinson disease and Prion disease [Erickson et al., 2005; Kim-Han et al., 2007; Sepulveda et al., 2016; Hettinghouse et al., 2018]. Available evidences indicate multiple distinct functional roles of PDIA3 under both physiological and disease states. In particular, under physiological conditions and during cellular stress, PDIA3 seems to play a role in cell protection against oxidative stress through its redox and chaperone activities, and it can prevent the development of diseases related to unfolded/misfolded proteins accumulation, such as Aβ [Ni et al., 2007; Ellerman et al., 2006; Plácido et al. 2014; Selinova et al., 2007; Erickson et al., 2005]. In line with the latter observation, it has been reported that diosgenin, a famous plant-derived steroidal saponin and structurally similar to the calcitriol, an endogen PDIA3 ligand [Nemere et al. 2012], acts as an exogenous activator of PDIA3, improving the object recognition memory deficit and reduce amyloid plaques and neurofibrillary tangles in the cerebral cortex and hippocampus of 5XFAD mice, an engineered mouse model of AD harboring five familial AD mutations [Tohda et al., 2012]. Likewise, diosgenin derivative, caprospinol (diosgenin 3-caproate), reduced amyloid deposits and improved memory dysfunction in Aβ1-42-infused AD model rats [Lecanu et al., 2010]. Furthermore, it has been demonstrated that PDIA3 expression levels significantly increased after Aβ1-42 treatment in HMO6 cells, an immortalized human microglial cell line, and in microglial cells from 5XFAD mouse brains [Yoo et al., 2015]. Collectively these observations highlighted that PDIA3 may play a crucial role in microglia activation during AD and that it may be a molecular target for AD treatment.

Although these promising observations, the data are sparse and mostly the relationship between alterations in PDIA3 expression and the development of AD neuropathology is still unclear.

1.3.2. PDIA3 and platelet aggregation

Platelets play a central role in the hemostatic process, including recognizing the site of injury, recruiting additional platelets by intercellular signaling, adhering to each other, and interacting with the coagulation cascade to form a haemostatic plug. Inappropriate platelet activation, and subsequent thrombus formation, is important in the clinical complications of arterial atherosclerosis and thrombosis. Platelets are activated by a variety of agents which act to recruit additional platelets to the site of injury, leading to the consolidation of the aggregate.

This activation process is initiated by the engagement of a range of specific cell surface receptors and associated to intracellular signaling pathways:

- ✓ Exocytosis of granular products: ADP, serotonin, calcium and fibrinogen are important in the recruitment of platelets to the site of injury.
- ✓ Expression of granular membrane proteins: Adhesive proteins (e.g., GPIb, P-selectin, CD63, and several integrins) have been shown to be present on the membranes of intracellular granules and are expressed on the surface of activated platelets.
- ✓ Eicosanoid formation: The arachidonic acid cascade is initiated, leading to Thromboxane A2 (TXA2) synthesis. TXA2 is a platelet agonist that plays a pro-aggregatory role.
- ✓ Surface expression of adhesive receptors: There is a conformational change in the αIIbβ3 integrin on the platelet surface from an inactive to an active configuration, exposing a fibrinogen and von Willebrand

Factor binding domain on the αIIbβ3 integrin that facilitates inter-platelet binding [McNicol and Israels, Critical Review, 2003].

PDIA3 is also present on the platelet surface and it is secreted by endothelial cells upon vascular injury and accumulates in the thrombus, where it regulates the activation and recruitment of other platelets [Holbrook et al., 2012]. In fact, it has been demonstrated through proteomic approach that PDIA3 is upregulated and released after GPVI activation, a glycoprotein receptor for collagen [Holbrook et al., 2012; Zhou et al., 2014]. Anti-PDIA3 antibody inhibits platelet aggregation, ATP secretion, calcium mobilization and activation of glycoprotein IIb/IIIa or fibrinogen receptor (αIIbβ3) in platelets stimulated with collagen-related peptide (CRP-XL), while platelet factor 4 (PF4) and P-selectin expression is minimally altered [Wang et al., 2013; Holbrook et al., 2012]. Genetically engineered mice lacking platelet-derived PDIA3 have prolonged tail bleeding times. PDIA3-null platelets reveal decreased platelet aggregation and decreased activation of αIIbβ3 [Wu et al., 2012]. β3 integrins pair with αIIb on the surface of platelets to create fibrinogen receptor αIIbβ3, the integrin activation is accompanied by several conformational changes that require a new pattern of disulfide bond formation [Zhou et al., 2014]. PDIA3 binding β3 integrin in thrombin-activated platelets is probably involved in platelets aggregation, due to its redox activity; however, the underlying mechanism is not completely understood. [Schulman et al., 2016].

1.4. Polyphenols

Flavonoids are a large class of polyphenolic compounds ubiquitous in plants and mostly present in fruits, vegetables and plant-based beverages

such as tea and wine [Perez-Jimenez et al., 2010]. Flavonoids are further sub-classified in to flavones, flavonols, iosflavones, flavanones, flavanols and anthocyanidins (Fig. 6) [Manach et al., 2004; Bravo 1998].

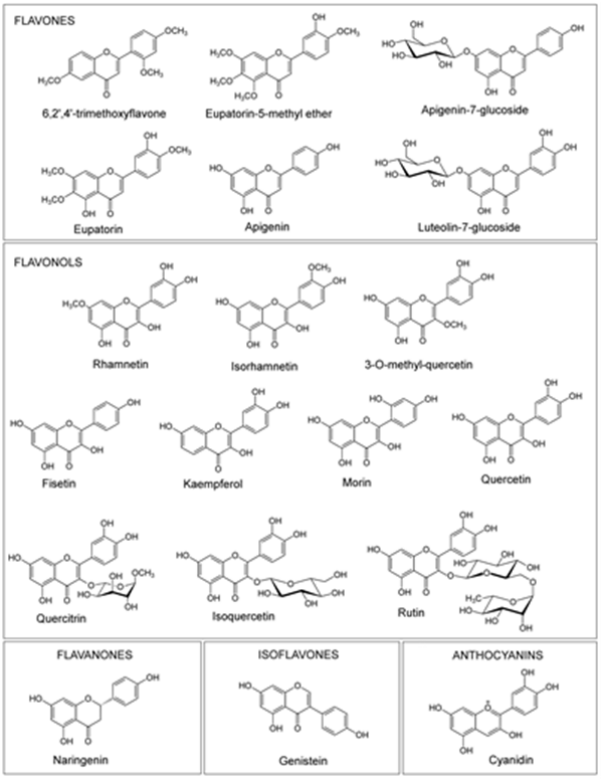

Figure 6. Molecular structure of tested flavonoids.

These physiologically active compounds have multiple well-known health beneficial effects. Many studies have suggested an association between consumption of flavonoids-rich food or beverages and the prevention of many degenerative diseases, including cancer, neurodegeneration and coronary heart disease and stroke [Woo et al., 2013; Hui et al., 2013; Hertog et al., 1993]. The protection offered by flavonoids is believed to be due to their antioxidant activity. The aromatic rings of the flavonoid molecule allow donation and acceptance of electrons from free radical species [Halliwell

2006]. In addition, many polyphenols regenerate the traditional antioxidant vitamins, vitamin C and vitamin E [Mandel et al., 2008] and act as metal chelators [Moridani et al., 2003]. It has been suggested that, in lower amounts, flavonoids as well as polyphenols may exert pharmacological activity within the cells, having the potential to modulate intracellular signaling pathways. Many polyphenols can induce antioxidant enzymes such as gluthathione peroxidase, catalase, superoxide dismutase, and inhibit the expression of enzymes such as xanthine oxidase, which is involved in the generation of free radicals [Alvarez-Suarez et al., 2011; Moskaug et al., 2005]. However, for many of them the molecular and cellular bases of these activities are not known yet.

Besides, data from literature indicate that several phytochemicals can be found in pomegranate fruits and can be a valuable aid in counteracting oxidative stress and preventing some major diseases. Pomegranate extracts have important biological properties, including anti-atherosclerotic, antioxidant, anti-inflammatory and antigenotoxics, properties that can help in preventing the development of chronic and debilitating diseases such as cardiovascular illnesses, type 2 diabetes and cancer [Jurenka 2008; Adams et al., 2006]. These activities have been attributed to the high content of phenolic compounds [Turrini et al., 2015; Medjakovic et al., 2013]. The nutraceutical properties of pomegranate are not limited to the edible part of the fruit; in fact, non-edible fractions of fruit and tree (e.g., peel, flower, …) contain even higher amounts of biologically active components. The peel of the pomegranate is rich in ellagitannins, such punicalagin, punicalin, gallagic acid, ellagic acid and glycosides (Fig. 7) [Akhtar et al., 2015; Masci et al., 2016].

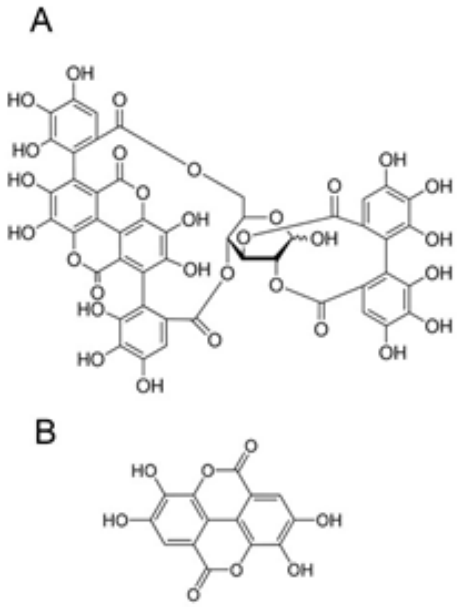

Figure 7. Chemical structure of punicalagin (A) and ellagic acid (B).

Punicalagin, a unique pomegranate compound of high molecular weight soluble in water, is the predominant ellagitannin. Punicalagin features important biological activities, including anti-inflammatory, hepatoprotective and anti-genotoxic activities. However, there are currently few studies on punicalagin biological efficacy [Seeram et al., 2006].

Chapter 2: Aim of the research

As above reported in Chapter 1, PDIA3 protein is a prominent member of the PDI family that has attracted a significant attention by the research community. It is also becoming increasingly evident that PDIA3 could be a pharmacological target in different pathological conditions, though the mechanisms in which it is involved are not completely understood. For this reason, my PhD project puts the spotlight on the PDIA3 involvement in disease processes, focusing on Alzheimer disease and platelet aggregation, and then characterizing its new features and roles in the development of the aforementioned diseases. At present, no selective compounds are known to modulate the PDIA3 biological functions. The discovery of specific PDIA3 interactors could be used in repressing or stimulating PDIA3 in biological model, thus providing useful information on PDIA3 functions.

2.1. Identification of specific natural PDIA3 interactors able to bind and modulate its activity

Polyphenol compounds display a wide range of biological effects, such as antioxidant, anti-inflammatory, antithrombotic, antiviral and antitumor activities [Vauzour et al., 2010]. They can act on different targets affecting regulation of a variety of pathways: cell signaling and cell cycle, free radical

scavenging, inhibition of angiogenesis, initiation of DNA repair mechanisms, apoptotic induction and inhibition of metastasis [Williams et al., 2004; Mandel et al., 2011; George et al., 2016]. However, for many of them the molecular and cellular bases of these activities are not known. PDIA3 is a multifunctional protein disulfide isomerase with a wide range of functions and involved in many biological processes such as cellular response to stress as well as in cancer and neurodegeneration [Hettinghouse et al., 2018]. In this regard, it is interesting to undertake a screening study for assessing the interaction and impact on PDIA3 protein activity of several types of natural compounds. The identification of specific ligands that can modulate and/or inhibit PDIA3 interaction with specific partners may be useful to selectively control cellular processes and signaling pathways involving PDIA3 and might offer new therapeutic tools.

This study, initially started in our lab by analyzing the major catechins present in the extracts of green tea [Trnkova et al., 2013], has been expanded to various classes of other natural compounds to assess their interaction and impact on PDIA3 protein activity. The binding of several polyphenols to PDIA3 were tested by fluorescence quenching assay. Their effects on the protein PDIA3 redox activity were also analyzed as well as their properties on a cellular model.

2.2. Assessment of PDIA3 involvement in platelet aggregation

In the last two decades, many research groups have focused on the development of new anti-aggregatory drugs in order to reduce the side effects or other draw-backs of older drugs. In fact, ASA (acetylsalicylic acid) is still

the drug of first choice for most relevant antiplatelet indications, but the major problem is 10-20% of clinical resistance. Furthermore, integrin αIIbβ3 (fibrinogen receptor) is another interesting target and the antagonists of fibrinogen or von Willebrand Factor (e.g., abciximab, tirofiban, …) have a high antiplatelet potency but need to be given in intravenous way [McNicol and Israels, Critical Review, 2003]. Considering that the availability of oral drugs is limited, the identification of new drug targets is of clinical interest. Previous study demonstrated that danshensu has anti-thrombotic properties inhibiting the activation of αIIbβ3 and blocking the PDIA3/αIIbβ3 complex on the platelet surface [Cui et al., 2015]. Published data support the PDIA3 role in platelet aggregation, though the intracellular mechanisms involved remain unclear. Several stimuli can trigger platelet aggregation, activating different intracellular pathways, as reported in Figure 8.

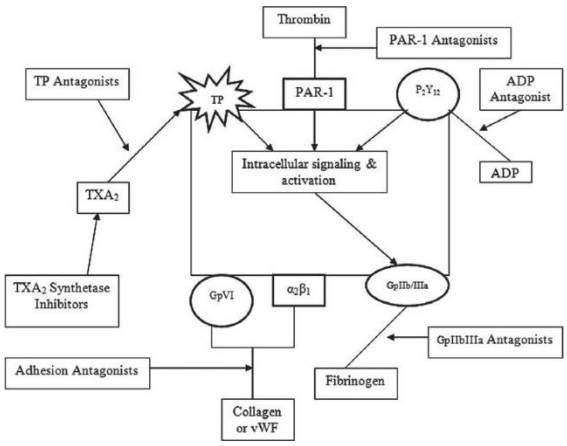

Figure 8. Schematic representation of different intracellular pathways involved in platelet aggregation.

It has been reported that PDIA3 can be released from platelets upon thrombin or collagen stimulation [Holbrook et al., 2010], demonstrating its possible involvement in their pathways. However, there are no evidences about the PDIA3 response via ADP or thromboxane A2 activation.

Hence, in my research, I used arachidonic acid and ADP as platelet activators, at different concentration, to investigate whether PDIA3 could be also involved in platelet aggregation through these ways.

2.3. PDIA3 expression is altered in the limbic brain regions of triple-transgenic mouse model of Alzheimer's disease

Evidences from the literature suggest that PDIA3 might have a role in AD pathogenesis [Erickson et al., 2005; Tohda et al., 2012], but its exact contribution is not clear. Therefore, we aimed to evaluate whether brain PDIA3 expression is altered in a triple transgenic model of AD (3×Tg-AD) in comparison with wild type littermates (Non-Tg). 3×Tg-AD mice, which harbor three mutant human genes [Oddo et al., 2003], mimic the critical aspects of AD-neuropathology observed in the human AD patients [Cassano et al., 2012; Romano et al., 2015; Scuderi et al., 2018]. Moreover, to investigate whether the temporal and regional patterns of such possible alterations might overlap with those of Aβ and tau pathology in this AD model, brain PDIA3 expression was analyzed at different ages [Oddo et al., 2003]. As a consequence, by studying the temporal expression of PDIA3 in the wild-type littermates, our study has also allowed us to analyze the impact of aging on PDIA3 levels. Our analyses were conducted on PDIA3 protein levels in 3×Tg-AD and Non-Tg mice at two different stages (mild and severe) of AD-like pathology. In particular, 6- and 18-month-old mice were analyzed by Dot-blot analysis and double-immunohistochemistry, followed by the semi-quantitative analysis of the respective signals. Amygdala,

hippocampus (dorsal and ventral), and entorhinal cortex, all brain regions strongly affected by the AD-neuropathology, were analyzed in this study. Then, the triple-immunohistochemistry was performed in order to investigate the sub-cellular localization of PDIA3. Taking together, the expression and the localization may help us to speculate the role and the importance of PDIA3 in both healthy and Alzheimer's condition.

Chapter 3: Materials and methods

3.1. Identification of specific natural PDIA3 interactors able to bind and modulate its activity

3.1.1. Chemicals

Punicalagin, ellagic acid, phosphate buffered saline (PBS), tris(2-carboxyethyl) phosphine (TCEP), dimethyl sulfoxide (DMSO), 4-(2-hydroxyethyl)-1-piperazineethanesulfonic acid (HEPES), dithiothreitol (DTT), oxidized glutathione (GSSG), eosin isothiocyanate, glutamine, sodium pyruvate, fetal bovine serum (FBS), penicillin and streptomycin and 19 different flavonoids (quercetin, 3-O-methyl-quercetin, isoquercetin, quercitrin, rutin, morin, rhamnetin, isorhamnetin, fisetin, apigenin, apigenin-7-glucoside, luteolin-7-glucoside, kaempferol, eupatorin, eupatorin-5-methyl-ether, genistein, narigenin, cyanidin and 6,2',4'-trimethoxyflavone were purchased from Sigma-Aldrich. EDTA (ethylenediaminetetraacetic acid) 0.5 M solution pH 8.0 was from IBI Scientific and sodium 3´- [1-(phenylaminocarbonyl)- 3,4- tetrazolium]-bis (4-methoxy- 6-nitro) benzene sulfonic acid hydrate (XTT) from Biotium. SYPRO Orange was from Invitrogen.

3.1.2. Protein expression and purification

Human recombinant PDIA3 was cloned and expressed in E. coli strain BL21 using the expression vector pET21 (Novagen) as previously described [Coppari et al., 2002]. The coding sequence for the second redox-active domain (a' domain, residues 377-505) was amplified by PCR as previously described and cloned in the expression vector pET29 (Novagen) [Grillo et al., 2007]. Recombinant proteins were expressed in E. coli strain BL21 and purified by ammonium sulphate fractionation, ion exchange and heparin chromatography [Grillo et al., 2007; Grillo et al., 2006]. Protein purification was evaluated by SDS-PAGE and concentration was determined spectrophotometrically (PDIA3 Ɛ280 reduced form = 44,810 $M^{-1}cm^{-1}$, a' domain Ɛ280 reduced form =14,400 M^{-1} cm^{-1}).

3.1.3. Fluorescence Quenching Measurements

The PDIA3-ellagitannins/flavonoids interaction was evaluated by fluorimetric titration. Fluorescence spectra were recorded using a SPEX-FluoroMax spectrofluorimeter (Horiba Scientific) from 300 to 500 nm with excitation at 290 nm using a 10 mm path length quartz fluorescence cuvette and under continuous stirring. The excitation and emission slits were both set to 5 nm and scan speed was 120 nm·min-1. First, PDIA3 was reduced adding 2 mM TCEP to 50 μM PDIA3 stock solution. Then, aliquots of freshly reduced PDIA3 (0.5 μM or 0.1 μM final concentration) was diluted in PBS containing EDTA 0.2 mM and DTT 0.1 mM, and titrated in quartz cuvette by stepwise additions, at 5 min time intervals, of individual flavonoid solution (1 mM in PBS/ethanol 50:50 v/v freshly prepared from a 20 mM stock solution in DMSO) or of ellagitannins solution (punicalagin 0.2 mM in

PBS freshly prepared from a 20 mM stock solution in water, ellagic acid 0.2 mM in PBS/ethanol 50:50 v/v freshly prepared from a 20 mM stock solution in DMSO). Most of tested flavonoids can absorb light at the excitation and emission wavelengths. To minimize the inner-filter effect, we limited the highest concentration reached in the titration test up to 10 µM. All experiments were carried out at 25°C. The blank spectra (polyphenol or flavonoids without protein) were recorded under the same experimental conditions and subtracted from the corresponding polyphenol-protein system to correct the fluorescence background. Fluorescence intensities recorded at 338 nm were used for quenching analysis and obtained data, as the average of at least three independent titration experiments.

3.1.4. Determination of Protein Disulfide Reductase Activity

Disulfide reductase activity of PDIA3 was monitored by sensitive fluorescent assay using dieosin glutathione disulfide (DiE-GSSG) as fluorogenic probe. DiE-GSSG is synthesized by the reaction of eosin isothiocyanate with oxidized glutathione (GSSG) according to the method of Raturi and Mutus [Raturi and Mutus 2007] with some modifications [Trnkova et al., 2013]. DiE-GSSG purification was determined in HPLC and its concentration was calculated spectrophotometrically (ε_{525}=88,000 $M^{-1}cm^{-1}$). Disulfide reductase activity was assayed in a reaction buffer containing 2 mM EDTA, 150 nM DiE-GSSG, 5 µM DTT and 1µM or 50 nM PDIA3 in PBS. The effect flavonoid (20 µM) and ellagitannins (0.2, 0.5, 2, 5 and 20 µ) effects were evaluated after 2 minutes incubation before the analysis. GSSG reduction was monitored for 3 minutes at 545 nm with excitation at 520 nm, at 25°C under continuous stirring. Reductase activity was calculated as the initial velocity in fluorescence increase. A better investigation on PDIA3

reductase activity was performed by DiE-GSSG titration (31nM to 1000 nM) in reaction buffer added with 20 nM final concentration of PDIA3 and DTT 5 μM. To assess the effect on the PDIA3 activity, before DiE-GSSG titration, PDIA3 20 nM was incubated with different concentrations of punicalagin (0.2, 0.5, 1, 2 and 5 μM) for 2 minutes. Values were fitted using the enzymatic kinetic equation on Graph Pad Prism 5.0 software (GraphPad Software, Inc.) to calculate Michaelis-Menten constant (K_m) and maximum velocity (V_{max}) for PDIA3 and their modifications after punicalagin treatment. Punicalagin inhibition constant (K_i) was determined using a Lineweaver-Burk plot or a Dixon plot analysis on Graph Pad Prism 5.0 software.

3.1.5. Isothermal titration calorimetry (ITC)

The thermodynamic analysis of PDIA3-punicalagin interaction was obtained using the MicroCal ITC (Malvern Instruments Ltd.). PDIA3 was extensively dialyzed and punicalagin was dissolved in the same buffer. The sample cell (0.2 ml) was filled with PDIA3 (25 μM) and the syringe with punicalagin (250 μM solution). Ligand solution was then injected into the cell in 19 aliquots of 2 μL for 4 s (the first injection was 0.4 μL for 0.8 s) with delay intervals between injections of 180 s. Syringe stirring speed was set to 800 rpm. PDIA3-punicalagin interaction was analyzed in both non-reducing and reducing condition. In the latter, 1 mM TCEP was added to protein and ligand solutions to ensure protein reduction. To correct the heat of dilution, titration of punicalagin into a buffer without PDIA3 was carried out. The thermodynamic data were processed with Origin 7.0 software

provided by MicroCal and used to calculate molar enthalpy, affinity constant and the stoichiometry of the reaction.

3.1.6. Cell Culture

Human bone marrow neuroblastoma cells (SH-SY5Y) were obtained from ATCC and PDIA3-silenced human bone marrow neuroblastoma cells (shPDIA3-SH-SY5Y) were obtained as follow. SH-SY5Y cells were cultured in 6-well plates and transfected with PDIA3 shRNA vector clone, obtained from the Mission shRNA library (Sigma), using Lipofectamine 2000 (Life Technologies) according to manufacturer's instructions. Six hours after transfection, medium was replaced with fresh medium. After 48 hours 1μg/mL puromycin was added to the cells to select stable transfected cell clones. Both neuroblastoma cell lines were grown to 60-70% confluence in Dulbecco's Modified Eagle's Medium Mixture F-12 Ham (DMEM F12) (Sigma-Aldrich) with 10% FBS, 1% w/v sodium pyruvate, 2mM glutamine, 100 U/mL penicillin and 100 mg/mL streptomycin at 37°C in 5% CO2 (1 μg/mL puromycin was added to shPDIA3-SH-SY5Y).

3.1.7. Cell Viability

To assess the cytotoxic effects of H_2O_2 and punicalagin, SH-SY5Y and shPDIA3-SH-SY5Y cells were seeded in 96-well plates and treated with different concentrations of H_2O_2 (0.05, 0.1, 0.2, 0.5, 1, 5 and 10 mM) or punicalagin (1, 2, 5, 10 and 20 μM) for 24 hours. Cell viability was measured using the XTT assay (Biotium) in accordance to the manufacturer's instructions. Briefly, the culture medium was removed and 125 μL/well of XTT solution was added to 96-well plates. After 3-6 hours incubation, the orange formazan dye, resulting from the conversion of the XTT yellow tetrazolium salt by metabolically active cells, was measured at 450 nm and

690 nm using Appliskan plate reader (Thermo Scientific). To assess H_2O_2-punicalagin co-treatment effects on cell viability, SH-SY5Y and shPDIA3-SH-SY5Y cells were seeded in 96-well plates and pre-treated for 4 hours with 20 μM punicalagin followed by H_2O_2 treatment (0.1, 0.2 and 0.5 mM) for 24 hours.

3.1.8. Cellular PDIA3 expression evaluated by Western Blotting

Western blot analysis on cellular extracts was used to evaluate the effect of different H_2O_2 treatments on PDIA3 expression in SH-SY5Y cells and to test PDIA3 silencing in shPDIA3-SHSY5Y cells. Cells were seeded in 6-well plates, subjected to different treatments and then lysated in RIPA Buffer. Extracted proteins were quantified by Bradford assay, resolved on SDS-PAGE in 10% TGX™ FastCast™ Acrylamide gels (BioRad), and then transferred to PVDF membranes (BioRad) using Trans-Blot® Turbo™ Transfer System (BioRad). Membranes were blocked with 1% w/v Bovine Serum Albumin (Sigma-Aldrich) in PBS. Membranes were incubated with anti-PDIA3 rabbit serum for 60 min, washed with TBST, and then incubated with peroxidase-conjugated anti-rabbit IgGs (Jackson ImmunoResearch) for an additional 60 min. After washing in TBST, the membranes were incubated with ECL substrates (Immunological Sciences) and the signal was detected by ChemiDoc™ Imaging Systems (BioRad). PDIA3 expression was analyzed using Image Lab™ Software (BioRad). Total proteins were used for normalization.

3.1.9. Statistical analysis

Fluorescence quenching constant (K_{SV}) values were given as means ± standard deviation and values of disulfide reductase activity were expressed in percentage of control sample ± relative standard deviation. All measurements were repeated at least three times. Dunnett's test was used to compare the obtained reductase activity data with the activity of the untreated protein and a p-value of < 0.01 was considered as statistically significant. Statistical comparisons were performed using ONE-WAY or TWO-WAY Analysis of Variance (ANOVA) and post hoc Bonferroni's test, with different H_2O_2 concentrations and punicalagin treatments as variables, using GraphPad Prism 5.0. The means of the data are presented with SEM. Statistical significance threshold was set to $p < 0.05$.

3.2. Assessment of PDIA3 involvement in platelet aggregation

3.2.1. Chemicals

Lyophilized Arachidonic Acid (AA), ADP and prostaglandin E1 (PGE1) were purchased from Roche Diagnostics GmbH and solubilized in ultrapure water (vehicle). EDTA (ethylenediaminetetraacetic acid) 0.5 M solution pH 8.0 was purchased from IBI Scientific.

3.2.2. Platelets isolations and activation

Human blood was drawn from consenting, healthy, medication-free individuals in accordance with Czech Republic ethical procedures. Platelets were prepared on the day of experimentation. Blood was sampled in heparinized tube and centrifugated at 1500 rpm (200g) for 8-15 minutes in

centrifuge CS4. The platelet rich plasma (PRP) was transferred into a new plastic tube using a pipette with wide orifice and without disturbing the buffy coat layer, in order to avoid contamination. Saline solution was added at 1:1 ratio (v/v), including PGE1 (1 μM final concentration) to prevent platelet activation. The tube was mixed very gently and then, centrifugated at 1000 rpm (100g) for 15-20 min in centrifuge CS4 at room temperature (with no brake applied) to pellet contaminating red and white blood cells. The supernatant was transferred into new plastic tube using a pipette with wide orifice. Platelets were pelleted by centrifugation at 5400 rpm (800 g) for 15–20 min at room temperature in centrifuge CS4. Platelet counts, by flow cytometry, were adjusted to the appropriate cell density by resuspension in saline ($5*10^7$ cell/ml). Platelet activation was induced by adding: AA (375, 150 and 50 μM final concentration), ADP (10, 5 and 2,5 μM final concentration), ultrapure water as vehicle (control) and PGE1 as negative control (1 mM final concentration). After 15 minutes platelet aggregation at 37°C, the activation was stopped by addition of EDTA-Na+ salt 1,45 mM final concentration. Platelets were centrifugated at 10000 rpm for 10 min. Stimulation of platelets using Arachidonic Acid, ADP was previous confirmed in Multiplate® Analyzer (Roche Diagnostics GmbH) with continuous stirring. Non-aggregatory conditions were detected by treating platelets with 1,45 mM EDTA-Na+ salt or with 1 mM PGE1.

3.2.3. PDIA3 Immunoblotting

Platelets were lysated in Lysis Buffer, vortexing and incubating on ice 15-30 min. After spin, pellets were resuspended, and proteins were precipitated with addition of 10% v/v trichloro acetic acid and centrifugated at 14000 rpm

for 20 min then, pellets were washed with 70% cold acetone. Dried pellets were dissolved in Sample Buffer and incubated at 30°C for 2 hours. Samples were resolved on SDS-PAGE in 10% TGX™ FastCast™ Acrylamide gels (BioRad) and transferred to PVDF membranes (BioRad) using Trans-Blot® Turbo™ Transfer System (BioRad). Membranes were blocked with 1% w/v Bovine Serum Albumine (Sigma-Aldrich) in PBS. Membranes were incubated with anti-PDIA3 rabbit serum for 60 min, washed with TBST, and then incubated with peroxidase-conjugated anti-rabbit IgGs (Jackson ImmunoResearch) for an additional 60 min. After washing in TBST membranes were incubated with ECL substrates (Immunological Sciences) and the signal was detected by ChemiDoc™ Imaging Systems (BioRad). PDIA3 expression was analyzed using Image Lab™ Software (BioRad). Total proteins were used for normalization.

3.2.4. PDIA3 immunoprecipitation from surrounding medium of aggregated platelets

Platelets ($5*10^7$ cells/ml) were stimulated using Arachidonic Acid, ADP and stimulation was terminated as previously described. Cell-free supernatants containing platelet-released proteins were obtained by centrifugation at 14000 rpm for 20 min at room temperature. Collected supernatants were incubated with 8 µg of Anti-PDIA3 antibody (Ab) for 1-1,2 hours at room temperature (RT) in rotation. Ab/protein complexes were added into 1 mg of Protein G-Dynabeads (Life Technologies), previously cleaned 2 times with Washing Buffer PH 7.4, and then incubated 2 hours at RT in rotation. The tubes were placed on the magnet and the unbound part was recovered. The Dynabeads®-Ab-protein complexes were washed 3 times with Washing Buffer PH 7.4 and transferred in a cleaned tube during last wash, to avoid co-elution of proteins bound to the tube wall. The Ab-protein

complexes were eluted, on the magnet, adding 50 mM Glycine pH 2.8 and incubating for 10 minutes at RT. The Ab-protein complexes were recovered and added with sample buffer 4X and Tris 1M pH 7.4 to equilibrate the PH. Samples were heated for 10 min at 70°C. The recovered Ab-protein complexes were resolved on SDS-PAGE in 10% TGX™ FastCast™ Acrylamide gels (BioRad) and subjected to western blotting against PDIA3 as above reported for total platelet extracted proteins.

3.2.5. Statistical analysis

Statistical comparisons were performed using ONE-WAY Analysis of Variance (ANOVA), with different concentrations treatment as variables, using GraphPad Prism 5.0. The means of the data are presented with SEM. Statistical significance threshold was set to $p < 0.05$.

3.3. PDIA3 expression is altered in the limbic brain regions of triple-transgenic mouse model of Alzheimer's disease

3.3.1. Animals

6- and 18-month-old male 3×Tg-AD mice and their male wild-type littermates (Non-Tg) were used in this study. The 3×Tg-AD mice harboring PS1M146V, APPswe, and taup301L transgenes were genetically engineered by LaFerla and colleagues at the Department of Neurobiology and Behavior, University of California, Irvine. Colonies of 3×Tg-AD and Non-Tg mice were established at the vivarium of the Puglia and Basilicata Experimental

Zooprophylactic Institute (Foggia, Italy). The 3×Tg-AD mice background strain is C57BL6/129SvJ hybrid and genotypes were confirmed from tail biopsy. The housing conditions were controlled (temperature 22° C, light from 07:00–19:00, humidity 50%–60%), and fresh food and water were freely available. The study was performed in accordance with guidelines released by the Italian Ministry of Health (D.L. 26/2014) and the European Directive 2010/63/EU. All efforts were made to minimize the number of animals used in the study and their suffering.

3.3.2. Protein isolation and Dot Blotting

After cerebral areas collection, tissues were lysated in Lysis Buffer and extracted proteins were quantified by Bradford assay. Directly, 5 µg of proteins were spotted on nitrocellulose membranes using a dot blot apparatus. Membranes were blocked with 1% w/v Bovine Serum Albumine in phosphate-buffered saline (PBS). Membranes were incubated with anti-PDIA3 rabbit (Millipore) for 60 min, washed with TBST and then incubated with anti-rabbit IgGs peroxidase-conjugated (Jackson ImmunoResearch), for an additional 60 min. After washing in TBST, membranes were developed by chemiluminescence with ECL substrates and the signal was detected by ChemiDoc™ Imaging Systems (BioRad). After stripping in glycine solution 0.1 M pH 3.0 for 15 min and neutralization with PBS, membranes were blocked with 1% w/v I-block in TBS for colorimetric detection. Then, membranes were incubated with anti-β-actin mouse (Sigma) for 60 min, washed in 1% w/v I-block and incubated with anti-rabbit IgGs alkaline phosphatase-conjugated (Jackson ImmunoResearch), for an additional 60 min. After washing in 1% w/v I-block in TBS solution, membranes were stained by colorimetric detection using alkaline phosphatase substrates (Quantace). The PDIA3 and β-actin protein expression was analyzed using

Image Lab™ Software (BioRad). The β-actin was used as house-keeping protein for normalization.

3.3.3. Double-fluorescence immunohistochemistry

Immunohistochemistry was performed using fluorescence-based revealing systems. For double fluorescence-based immunohistochemistry, 20-µm-thick brain coronal sections were obtained using a cryostat (Microm™ HM550, Thermo Fisher Scientific, MI, USA), and were mounted on positively charged microscope slides, which were stored at -20° C until further processed. The brain sections were incubated with 90% formic acid for 7 min followed by PBS washes. Then brain sections were blocked with a PBS solution containing 5% normal goat serum and 0.3% Triton X-100 followed by overnight incubation with purified anti-β-amyloid/APP 1-16 primary antibody (BioLegend®) and with PDIA3 rabbit polyclonal antiserum (Millipore) at 4°C. After removing primary antibodies, the slides were incubated with both secondary antibodies Alexa Fluor 594 goat anti-rabbit IgG and Alexa Fluor 488 goat anti-mouse IgG for 1.5 h at room temperature. After washing off excess secondary antibodies, the slides were incubated with Hoechst (Sigma). After washing excess Hoechst with PBS, the slides were mounted using an anti-fade medium (Fluoromount, Sigma-Aldrich). Furthermore, the specificity of the immunofluorescent staining for Aβ/APP and PDIA3 was confirmed on a separate set of slides by omitting the primary antibodies.

3.3.4. Triple-fluorescence immunohistochemistry

For triple fluorescence-based immunohistochemistry, each 20-µm-thick brain coronal section were mounted on a microscope slide and stored at –

20°C. The slides were washed several times with PBS/Triton 0.1%. Subsequently, the slides were incubated for 20 minutes into a sodium citrate buffer pre-heated at 95°C. After the heat-induced antigen retrieval step, the slides were cooled at room temperature in a water bath and washed with PBS/Triton 0.1%. Before the incubation with primary antibodies, the brain sections were blocked with a solution containing 10% BSA and PBS/Triton 0.3%. Thereafter, the slides were incubated for 16 h at 4°C with the primary antibodies: GFAP chicken polyclonal antibody (Abcam), NeuN mouse monoclonal antibody (Abcam) and PDIA3 rabbit polyclonal antiserum (Millipore). After washing off excess antibodies, sections were incubated with secondary antibodies: DyLight 350 goat anti-chicken, Alexa Fluor 488 goat anti-mouse IgG and Alexa Fluor 594 goat anti-rabbit IgG for 1.5 h at room temperature. After washing off excess secondary antibodies, the slides were mounted with the anti-fade medium. Even in this case, the specificity of the immunofluorescent staining for GFAP, NeuN and PDIA3 was confirmed by the omission of primary antibodies in another set of brain sections. Fluorescence-based immunolabeled slides were observed using a Nikon 80i Eclipse microscope equipped with a Qicam 12-bit Fast 1394 digital camera, and NIS-elements BR software (Nikon, Tokyo, Japan).

3.3.5. Statistical analysis

The correlation analysis between Aβ and PDIA3 protein levels was performed on the respective optical densities measured on double immunofluorescent slices and expressed as percentage of those measured in 6-month-old Non-Tg mice, by using the Pearson correlation test. The Aβ/APP and PDIA3 optical density values were analyzed by two-way ANOVA, with genotype (3×Tg-AD vs Non-Tg) and age (6 months of age vs 18 months of age) as between-subject factors. Tukey’s honestly significant

difference test was used for multiple post hoc comparisons, when required. Statistical significance threshold was set at $p < 0.05$.

Chapter 4: Results

4.1. Identification of specific natural PDIA3 interactors able to bind and modulate its activity

4.1.1. Study of the natural compounds-PDIA3 interaction by fluorescence analysis

We started a screening analysis to find molecules which specifically bind PDIA3. Such substances could be useful to modulate the biological functions of PDIA3. In this study, the interaction of different flavonoids with PDIA3 and their effects on protein reductase activity were evaluated. Two polyphenols (i.e., punicalagin and ellagic acid) and a number of flavonoids (e.g., flavones, flavonols and several derivates), which differ in terms of skeleton structure as well as hydroxyl-, methoxyl- and other substituted groups, were analyzed (Fig. 6, 7).

The interaction was investigated by quenching analysis of PDIA3 intrinsic fluorescence mainly due to the presence of three tryptophan residues. They differ from each other in solvent or quencher accessibility and can unequally contribute to the protein fluorescence. One tryptophan residue (W279) is buried in a hydrophobic pocket in the b´ domain, whereas the others (W56

and W405) are present on the protein surface close to the thioredoxin-like active sites within a and a' domains, respectively. Quenching analysis was performed on PDIA3, in the reduced form, by adding stepwise increasing concentration of each molecules and recording the protein fluorescence spectra. For some flavonoids the analysis was extended to isolate a' domain (1 μM), always in the reduced form. Since all molecules can absorb light in the range of used excitation and emission wavelengths, in these experiments the highest final polyphenols concentration was kept stable to 10×10^{-6} M in order to limit their absorbance. Quenching effect on protein as well as Stern-Volmer quenching constants (K_{SV}) were calculated from the fluorescence intensities at 338 nm of protein alone (F_0) and in the presence of increasing concentration of each ligand molecule (F) using the Stern-Volmer equation [Lakowicz 2006]:

$$\frac{F_0}{F} = 1 + K_{SV}[L]$$

where L is the ligand concentration. For each ligand molecule, the Stern-Volmer quenching constant was obtained by linear regression of plots of $F_0/_F$ versus [L].

Representative fluorescence spectra of PDIA3 in the presence of increasing concentration of punicalagin are showed in Figure 9.

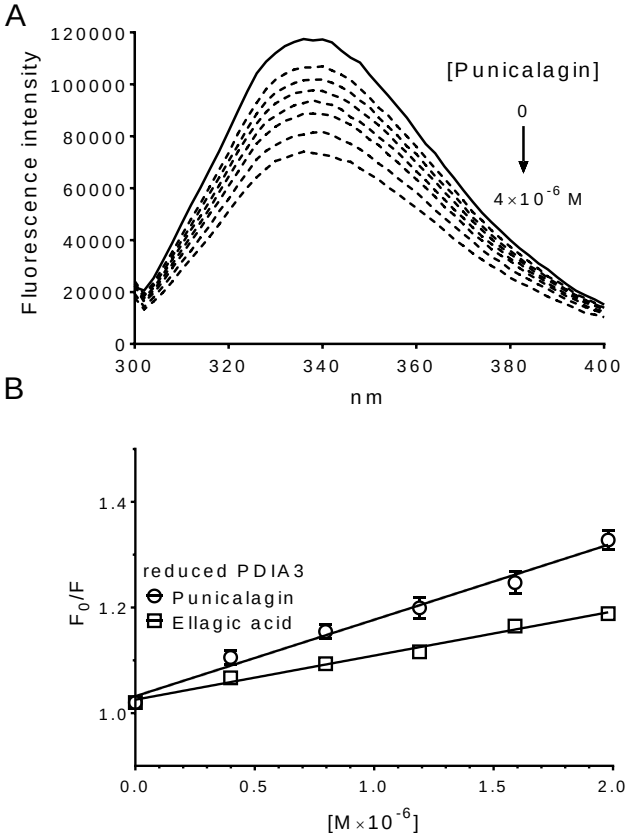

Figure 9. Protein fluorescence quenching analysis of PDIA3 in the presence of punicalagin. Protein fluorescence quenching analysis of PDIA3 in the presence of punicalagin (A) Fluorescence quenching spectra of reduced PDIA3 alone (solid line) and after stepwise addition of punicalagin (A) (dotted line) (pH 7.4, 25°C, and λ_{ex} = 290 nm,). (B) Stern-Volmer plot of quenching data of reduced PDIA3 in the presence of increasing concentrations of punicalagin and ellagic acid. Data represent the mean of at least three independent experiments and error bars indicate SEM.

A different degree of quenching was observed in presence of tested molecules. The decrease of fluorescence may indicate that the microenvironments of tryptophan residues in PDIA3 were altered due to the interaction with tested compounds. No evident spectral shift was noticed in

fluorescence spectra of PDIA3 after the additions of all tested molecules, suggesting that these substances do not induce any evident change in protein conformation.

This interaction should involve regions of the protein near the two tryptophan residues, W56 and W405, more exposed to the solvent and close to the redox active sites.

The apparent binding constants (K_b) was calculated using the equation described by Bi and colleagues [Bi et al., 2005]:

$$\log\left(\frac{F_0 - F}{F}\right) = n \log K_b - n \log\left(\frac{1}{[L_t] - n(F_0 - F)[L_t]/F_0}\right)$$

where F_0 and F are the fluorescence intensities at 338 nm before and after the addition of the quencher, [L] and [P_t] are the ligand and the total protein concentrations, respectively. The number of binding sites (n) and the binding constant (K_b) were obtained by plotting log ((F_0 – F)/F) versus log(1/([L_t]-n (F_0 – F)[P_t]/F_0)) using the reiterative calculation process described by Sun et al. [42], assuming a similar affinity for each binding site. The dissociation constant was calculated from the binding constant (K_d = 1/K_b).

The estimated K_{SV}, K_b and K_d values that characterize the interaction of PDIA3 with tested compounds are summarized in Table 1.

	K_{SV} (M^{-1})	Kq ($M^{-1}s^{-1}$)	K_b (M^{-1})	K_d (M)
Flavone				
Trimethoxyflavon	22209 ± 484	$2{,}22\cdot10^{12}$	18123	$55{,}2\cdot10^{-6}$
Eupatorin-5-methylether	90016 ±1875	$9{,}00\cdot10^{12}$	90440	$11{,}1\cdot10^{-6}$
Eupatorin	89362 ±688	$8{,}94\cdot10^{12}$	96729	$10{,}3\cdot10^{-6}$
Apigenin	54332 ±1185	$5{,}43\cdot10^{12}$	58739	$17{,}0\cdot10^{-6}$
Apigenin-7-glucoside	43961 ±673	$4{,}40\cdot10^{12}$	47287	$21{,}1\cdot10^{-6}$
Luteolin-7-glucoside	31601 ±484	$3{,}16\cdot10^{12}$	34557	$28{,}9\cdot10^{-6}$
Flavanone				
Naringenin	16900 ±352	$1{,}69\cdot10^{12}$	17295	$57{,}8\cdot10^{-6}$
Isoflavone				
Genistein	22953 ±435	$2{,}30\cdot10^{12}$	24409	$41{,}0\cdot10^{-6}$
Flavonol				
Rhamnetin	28462 ±295	$2{,}85\cdot10^{12}$	30110	$33{,}2\cdot10^{-6}$
Isorhamnetin	36109 ±1271	$3{,}61\cdot10^{12}$	32516	$30{,}8\cdot10^{-6}$
3-O-methyl-quercetin	41110 ±794	$4{,}11\cdot10^{12}$	45719	$21{,}9\cdot10^{-6}$
Fisetin	33164 ±542	$3{,}32\cdot10^{12}$	36862	$27{,}1\cdot10^{-6}$
Kaempferol	28423 ±982	$2{,}84\cdot10^{12}$	26000	$38{,}5\cdot10^{-6}$
Morin	24063 ±265	$2{,}41\cdot10^{12}$	25613	$39{,}0\cdot10^{-6}$
Quercetin	46226 ±1406	$4{,}62\cdot10^{12}$	38987	$25{,}6\cdot10^{-6}$
Quercitrin	29211 ±483	$2{,}92\cdot10^{12}$	32288	$31{,}0\cdot10^{-6}$
Isoquercetin	25738 ±367	$2{,}57\cdot10^{12}$	29073	$34{,}4\cdot10^{-6}$
Rutin	45197 ±465	$4{,}52\cdot10^{12}$	45527	$22{,}0\cdot10^{-6}$
Anthocyanin				
Cyanidin	29761 ±635	$2{,}98\cdot10^{12}$	29257	$34{,}2\cdot10^{-6}$
Ellagitannin				
Punicalagin	14115 ±4803	$14{,}9\cdot10^{12}$	120100	$8{,}3\cdot10^{-6}$
Ellagic Acid	74145 ± 3140	$7{,}4\cdot10^{12}$	40800	$24{,}5\cdot10^{-6}$

Table 1. The estimated K_{SV}, K_b and K_d values of the interaction of PDIA3 with tested compounds**.** Data were calculated from fluorescence quenching analysis using 0.5 or $0.1*10^{-6}$ M PDIA3 in reduced conditions (pH 7.4, 25°C) and increasing concentration (0 to $10*10^{-6}$ M) of different molecules. K_{SV} are reported as mean and standard deviation of at least three independent experiments. The number of binding sites (n), the binding constant (K_b) and the dissociation constant (K_d) were estimated using the equation described by Bi et al. [Bi et al., 2005] and the reiterative calculation process described by Sun et al. [Sun et al., 2010].

Although the protein can bind most of the tested substances, with an estimated dissociation constant within the 10^{-5} M range, some of them showed a better affinity. Molecules characterized by the highest binding constants are punicalagin and ellagic acid with a K_d around $1.0x10^{-6}$ M. For

some flavonoids, the binding analysis was extended to the isolated a' domain. Similar values for the binding constants were estimated, with some flavonoids showing a slightly better affinity for the whole protein respect to the isolated domain (data not shown).

4.1.2. Effect of natural compounds on the PDIA3 redox activity

To verify whether the interaction between flavonoids and PDIA3 may have an effect on protein functions, the disulfide reductase activity was tested using DiE-GSSG as fluoregenic substrate. For most of the molecules analyzed the effect on the redox activity of the protein was negligible. However, some molecules, in particular punicalagin but also the flavones eupatorin and eupatorin-5-methyl ether, showed an evident inhibitory effect. Others, such as morin, quercetin and cyanidin, had a less marked inhibition, approximately 20 (Fig. 10).

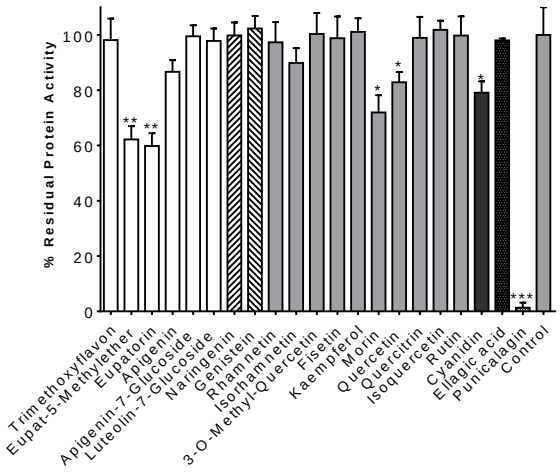

Figure 10. Comparison of polyphenols effect (at 20 μM) on PDIA3 reductase activity. Plots are displayed as mean and standard deviations of at least six independent measurements.

Data were analyzed by Dunnett's test comparing PDIA3 activity in presence of each molecules with the activity of untreated protein. Significant differences are marked with asterisks (*p < 0.5, **p <0.01, *** p < 0.001).

Considering the significant differences reported between punicalagin and all the molecules and its better affinity to PDIA3, we decided to better investigate this interaction. PDIA3 redox activity was tested in presence of different punicalagin concentrations and results were analyzed as logarithmic dose-response obtaining a half maximal inhibitory concentration (IC50) of about 1×10^{-6} M (Fig. 11).

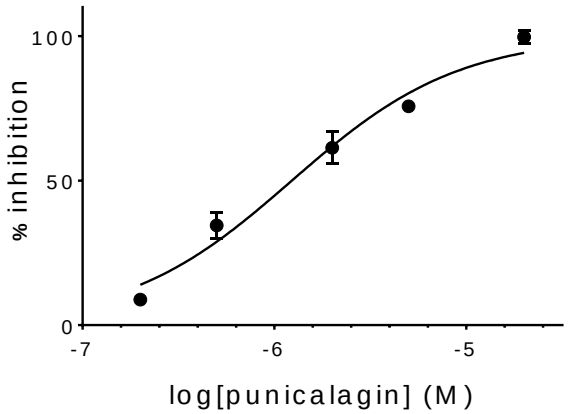

Figure 11. Logarithmic dose-response curve for punicalagin. Reductase activity of PDIA3 was recorded in the presence of increasing concentration of punicalagin and DiE-GSSG as substrate. Activity was calculated as the fluorescence increase of DiE-GSSG after enzymatic reduction at a fixed time. Percentage of inhibition was referred to PDIA3 reductase activity in absence of punicalagin. Data represent the mean of at least three independent measurements and error bars indicate SEM. [PDIA3] = 50×10^{-9} M, [DiE-GSSG] = 200×10^{-9} M, [punicalagin] = 0.2×10^{-6} M to 20×10^{-6} M.

Better characterization of punicalagin profile as PDIA3 inhibitor was performed changing both substrate and punicalagin concentrations. Data were analyzed using Lineweaver-Burk or Dixon plots (Fig. 12): it seems that punicalagin acts mainly as non-competitive inhibitor with a K_i of 0.39×10^{-6} M.

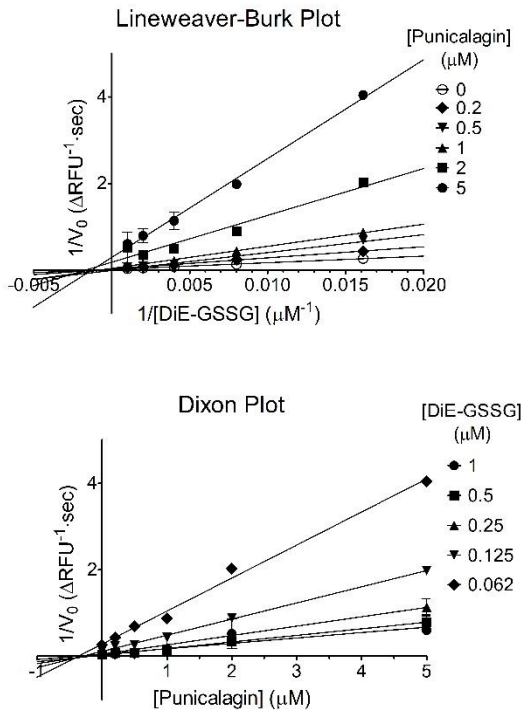

Figure 12. Kinetic analysis of punicalagin. Lineweaver-Burk (A) and Dixon (B) plots were obtained analyzing the PDIA3 reductase activity in the presence of increasing concentration of substrate (DiE-GSSG) and punicalagin as inhibitor. PDIA3 activity was measured as the initial velocity recording the fluorescence increase that result from DiE-GSSG reduction. Data represent the mean of at least three independent measurements and error bars indicate SEM. [PDIA3] = 20×10^{-9} M, [DiE-GSSG] = 62×10^{-9} M to 1000×10^{-9} M, [punicalagin] = 0 to 5×10^{-6} M.

On the basis of our data punicalagin-PDIA3 interaction should involve regions of the protein near the two tryptophan residues, W56 and W405, more exposed to the solvent and close to the active sites. Punicalagin does not seem to be affecting the binding of DiE-GSSG as substrate behaving mainly as non-competitive inhibitor. More probably punicalagin affects the conformational changes of cysteine residues at the active site that are required for the enzymatic activity.

4.1.3. Punicalagin effects on PDIA1

PDIA3 and the homologous isoform PDIA1, although similar in overall domain structure and active-site motifs, carry out different functions that are the result of specialized substrate binding properties. These differences are mainly related to the C-terminal domains b' and a' that show the lowest homology between the two isoforms [Klappa et al., 1998; Pirneskoski et al., 2001]. Then, we decided to compare the punicalagin effects on redox activity of PDIA1 and PDIA3 proteins. First, human recombinant PDIA1 was cloned and expressed in E. coli strain DH5α using the expression vector PET23-b (kindly donated by Professor Ruddock L. from Oulu University, Finland). Recombinant protein was expressed in E. coli strain BL21 and purified by nickel chromatography due to the presence of terminal His-Tag. Protein purification was evaluated by SDS-PAGE and concentration was determined spectrophotometrically (PDIA1 ε_{280} reduced form = 45,567 $M^{-1}cm^{-1}$). The disulfide reductase activity of PDIA1 was monitored in the same experimental conditions, as reported above for PDIA3. Obtained data, reported in Figure 13, demonstrated that the PDIA3 redox activity respect to PDIA1, was already inhibited at low concentrations of punicalagin. Then, these preliminary data confirm that punicalagin is more specific for PDIA3, but other experiments must be performed to provide further evidence that confirm our hypothesis.

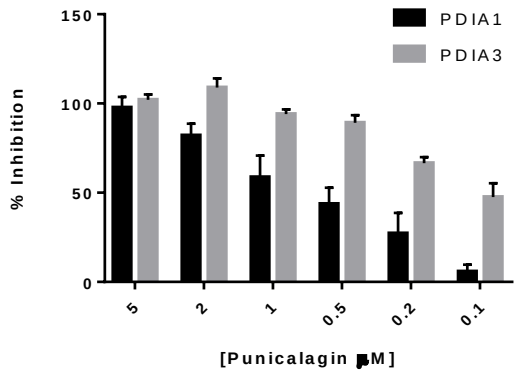

Figure 13. Comparison of punicalagin effects on PDIA3 and PDIA1. Reductase activity of PDIA3 and PDIA1 was recorded in the presence of DiE-GSSG, as substrate, and increasing concentration of punicalagin. Activity was calculated as the fluorescence increase of DiE-GSSG after enzymatic reduction at a fixed time. Percentage of inhibition was referred to PDIA3 or PDIA1 reductase activity in absence of punicalagin. Data represent the mean of at least three independent measurements and error bars indicate SEM.

4.1.4. Calorimetric analysis of Punicalagin-PDIA3 interaction

To further investigate the interaction of punicalagin with PDIA3, we decided to use calorimetric techniques to measure the thermodynamic parameters associated with the formation of the complex. The formation of the punicalagin-PDIA3 complex was analyzed by isothermal titration calorimetry (ITC). The measure of the absorbed or released heat, by protein titration with a ligand at constant temperature, yields the stoichiometry of the reaction, the binding enthalpy, and the affinity constant. ITC analysis was performed by adding punicalagin to PDIA3, in reducing condition and results are reported in Figure 14 and Table 2.

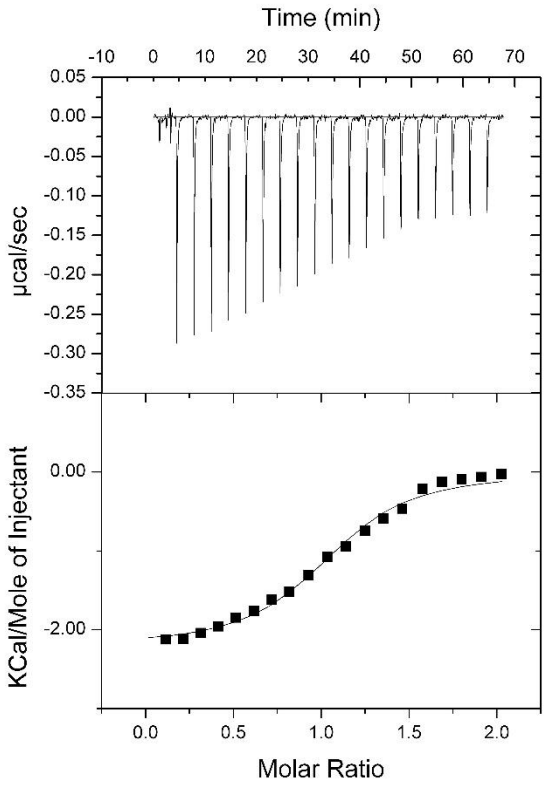

Figure 14. Binding of punicalagin to PDIA3 analyzed by ITC. Punicalagin-PDIA3 interaction was analyzed by isothermal titration calorimetry. 2 µl aliquots of punicalagin (250×10^{-6} M) were stepwise added to sample cell (0.2 ml) containing PDIA3 solution (25×10^{-6} M) and heat variation was recorded. Data were processed with software provided by MicroCal. Upper panel: raw data of a representative experiment of punicalagin-PDIA3 interaction. Lower panel: corresponding binding isotherm fitted according to the "one binding site" model.

	***Kd* (M)**	**Δ*H* (cal/mol)**	**TΔ*S* (cal/mol)**
Reduced PDIA3	1.2×10^{-6}	-1.1×10^{3}	6.9×10^{3}

Table 2. Thermodynamic data of punicalagin-PDIA3 interaction. Affinity constant (K_d), molar enthalpy (ΔH) and entropy (TΔS) of the reaction at 25°C were calculated processing data obtained from the isothermal titration. PDIA3 (25×10^{-6} M) was analysed in reduced and non-reduced conditions.

Thermodynamic analysis confirms the binding affinity of punicalagin to PDIA3 with a K_d of 1.2×10^{-6} M. ΔH always shows a negative value (-1.1 Kcal/mol) while TΔS is positive (6.9 Kcal/mol) at 25 °C, thus indicating that both entropy and enthalpy contribute to reduce the system's free energy. This result suggests non-covalent interactions formation at the binding interface, including van der Waals contacts, hydrogen bonds and other polar and apolar interactions. However, the high positive TΔS value indicates that the solvent entropy gain, arising from the redistribution of water molecules, plays an important role.

Punicalagin-PDIA3 interaction does not seem to be an enthalpy driven process but better fits with a lock-and-key model, which has been described as an entropy-dominated binding process. Since it is difficult to distinguish which factor, entropy or enthalpy, contributes more to ligand-protein interaction, a conformational selection binding model cannot be excluded [Du et al., 2016].

4.1.5. PDIA3 responses to H_2O_2 exposure in SH-SY5Y cells

PDIA3 has been thought to be a participant in the mechanisms of cell protection against oxidative stress through its redox and chaperone activities. PDIA3 could efficiently help in reducing the intracellular level of oxidized proteins produced upon cell exposure to damaging agents and in preventing the accumulation of misfolded or self-aggregating proteins. We previously reported that the overexpression of PDIA3 in HeLa cells resulted in a marked protective effect against the oxidative insult of hydrogen peroxide [Grillo et al., 2006].

To provide information on *in vitro* effects of punicalagin, we used, as cellular model, the neuroblastoma cell line SH-SY5Y. First, punicalagin effect on cell viability was assessed and no cytotoxic activity was observed using concentrations of punicalagin up to 20 μM (data not shown). Then, cell viability is progressively reduced after exposition to increasing concentrations of hydrogen peroxide (Fig. 15 A). Although cell response to oxidative stress can involve several activities, we focused on PDIA3 to test its behavior upon hydrogen peroxide exposition. Western blot analysis showed an increase of PDIA3 levels in stressed cells that becomes significant at the highest concentration of hydrogen peroxide tested (Fig. 15 B). Our results seem to confirm a PDIA3 involvement in cellular response to oxidative stress in this neuroblastoma cell line.

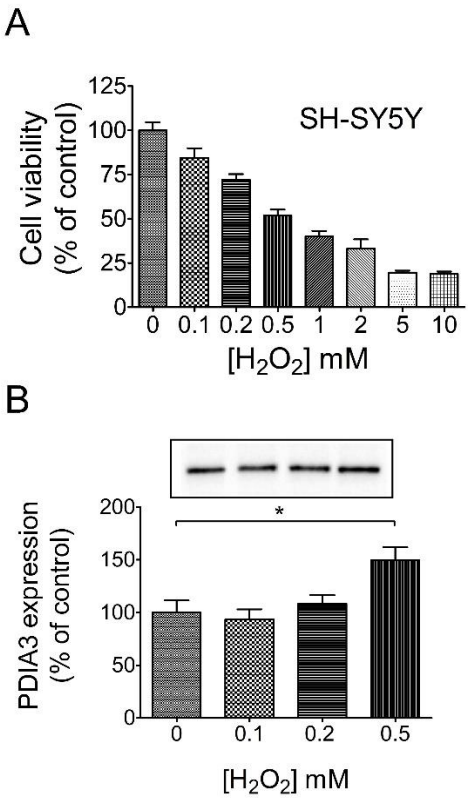

Figure 15. SH-SY5Y cell response to oxidative stress. SH-SY5Y cell were stressed by treatment with hydrogen peroxide at different concentration. (A) Cell viability was assessed by XTT assay. (B) PDIA3 expression levels were measured by western blot analysis on cell extracts. Inset shows a representative western blot image. Cell viability and PDIA3 expression levels are expressed as percentage of measured data in stressed cells compared to those measured in unstressed cells (control) and referred to the same number of cells. Data represent the mean of at least three independent measurements and error bars indicate SEM. Data were subjected to statistical analysis and significant differences ($p < 0.05$) are marked with asterisks.

4.1.6. Punicalagin increases cell sensitivity to oxidative stress in SH-SY5Y respect to shPDIA3-SH-SY5Y cells

Considering the above results, we tested whether punicalagin may affect the cell sensitivity to hydrogen peroxide treatment in the neuroblastoma cell model. Therefore, cells were preincubated with or without punicalagin and then subjected to oxidative stress by hydrogen peroxide treatment. Results show that the viability of cells exposed to different concentrations of hydrogen peroxide in the presence of punicalagin is always significantly lower compared to cells treated with hydrogen peroxide alone (Fig. 16 A). Supporting the idea that PDIA3 is one of the proteins involved in oxidative stress response, we can speculate that the observed punicalagin effect on neuroblastoma cell viability may be related to the above demonstrated ability of punicalagin to bind and modulate PDIA3 redox activity. Hence, we analyzed hydrogen peroxide cell sensitivity in PDIA3-silenced neuroblastoma cells under the same experimental conditions of wild-type cells, pre-treated with or without punicalagin. First, the silencing of PDIA3 was assessed comparing PDIA3 expression level in wild type cells (wtSH-SY5Y) and corresponding silenced cells (shPDIA3-SH-SY5Y) (Fig. 16 B). Figure 16 C shows that the presence or absence of punicalagin does not influence the cell viability in PDIA3-silenced cells exposed to hydrogen peroxide. A less evident effect of punicalagin can be observed only at the highest concentration of hydrogen peroxide and this can be explained since the silencing of PDIA3 in shPDIA3-SH-SY5Y cells was not fully achieved.

Obtained data provide evidences that punicalagin increases the cell sensitivity to hydrogen peroxide in neuroblastoma cells but this effect is drastically reduced in PDIA3-silenced cells. This suggests that punicalagin effect can be, at least, partially due to its ability to influence PDIA3 redox

activity, thus modulating the cellular sensitivity to hydrogen peroxide. We cannot exclude that other proteins, such as peroxidases and other redox enzymes, can be involved in cell response to oxidative stress and their activity can be modified by punicalagin. However, our preliminary results suggest that punicalagin acts as a PDIA3 ligand that can modulate its reductase activity also in a biological model.

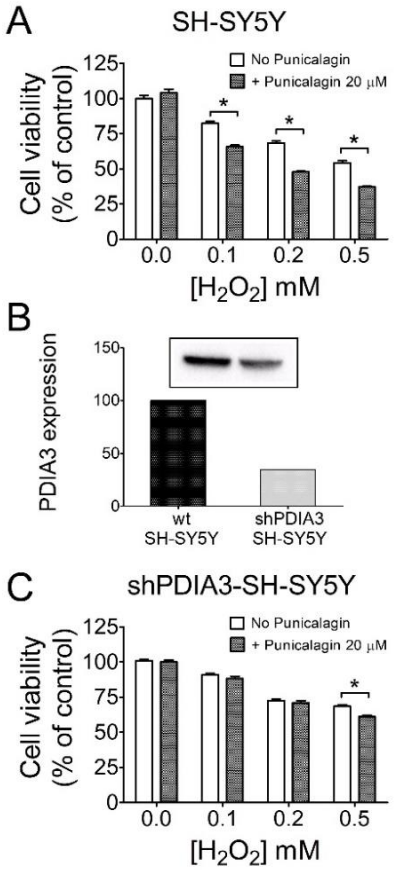

Figure 16. Punicalagin increases cell sensitivity to oxidative stress in SH-SY5Y respect to shPDIA3-SH-SY5Y cells. SH-SY5Y (A) and shPDIA3-SH-SY5Y (C) cells were stressed by treatment with hydrogen peroxide at different concentration in absence or presence of punicalagin 20×10^{-6} M. Cell viability was assessed by XTT assay. Cell viability is expressed

as percentage of measured data in stressed cells compared to that measured in unstressed cells (control) and referred to the same number of cells. Data were subjected to statistical analysis and significant differences ($p < 0.05$) are marked with asterisks. (B) PDIA3 silencing was assessed comparing PDIA3 expression level in wtSH-SY5Y and corresponding silenced cells (shPDIA3-SH-SY5Y). PDIA3 expression levels were measured by western blot analysis on cell extracts and expressed as percentage of measured data in wild type cells. Inset shows a representative western blot image.

4.2. Assessment of PDIA3 involvement in platelet aggregation

4.2.1. PDIA3 protein levels after platelet stimulation

To assess the PDIA3 protein basal level and the effects of vehicle administration on platelets, protein extracts from whole lysated platelets and treated-platelets with ultrapure water (control), were resolved by SDS-PAGE and then, subjected to western blot assay. It was also detected PDIA3 protein level under platelet aggregation inhibition following 1 mM PGE1 stimulation.

As reported in Figure 17, PDIA3 protein basal levels were not affected by vehicle (ultrapure water) treatment as well as to 1mM PGE1 stimulation. Indeed, no significant changes have been reported comparing whole lysated platelets to control or non-aggregated platelets (Fig. 17).

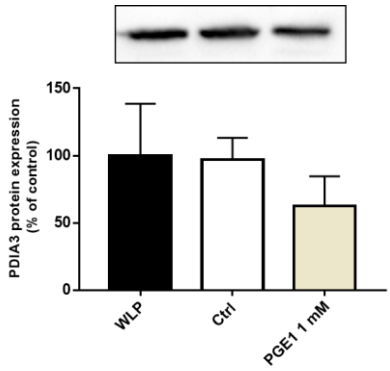

Figure 17. PDIA3 protein levels on platelet extracts. PDIA3 protein levels are expressed as percentage of measured data in treated-platelets with vehicle (control) and non-aggregated platelets compared to those measured in whole lysated platelets and referred to the same number of platelets ($5*10^7$/ml). Inset shows a representative western blot image. Data represent the mean of at least three independent measurements and error bars indicate SEM.

Hence, PDIA3 protein levels were detected after platelet aggregation induction for 15 min adding AA (Arachidonic Acid) or ADP at different final concentrations. Western blot analysis shows that AA and ADP induced a PDIA3 decrease in a dose-dependent manner, that becomes significant at 375 µM AA and 5 µM ADP, respectively (Fig. 18 A-B).

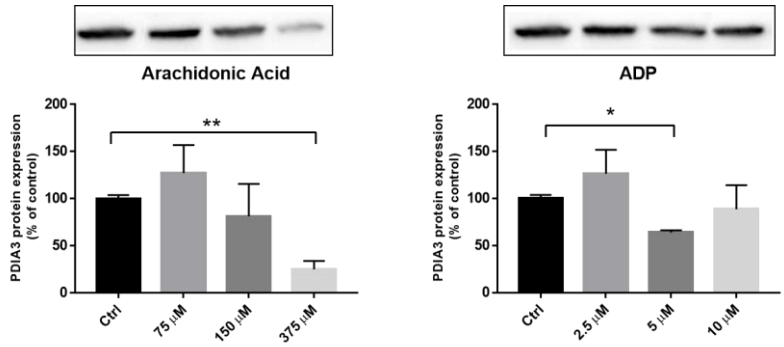

Figure 18. PDIA3 protein levels on platelet extracts. PDIA3 protein levels are expressed as percentage of measured data in stimulated platelets with increasing concentration of A) AA

B) ADP compared to those measured in treated-platelets with vehicle (control) and referred to the same number of platelets (25* 10^6/ml). Inset shows a representative western blot image. Data represent the mean of at least three independent measurements and error bars indicate SEM. Data were subjected to statistical analysis and significant differences ($p < 0.05$) are marked with asterisks.

4.2.2. PDIA3 can be released under arachidonic acid and ADP treatment

Previous studies have demonstrated that PDIA3 can be released into the surrounding media from activated platelets with thrombin or CRP-XL [Holbrook 20]. In order to investigate whether PDIA3 can be also released from platelets following stimulation with AA and ADP, platelets were activated and then removed from the cell suspension by centrifugation. Western blotting of platelet surrounding media shows that both AA and ADP can induce the release of PDIA3 from activated platelets (Fig. 19). It was also observed that both rested and PGE1-treated platelets released PDIA3, but since the experiments were performed starting from the same number of platelets (25*10^6/500µl), it can be speculated that the amount of secreted PDIA3 increased after AA and ADP stimulation.

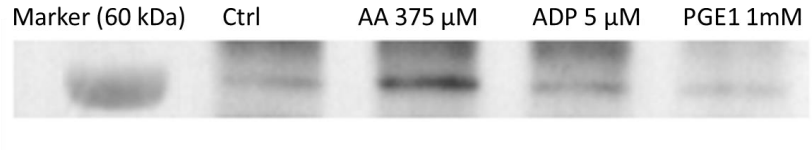

Figure 19. A representative western blot image of secreted PDIA3 from differently stimulated platelet. PDIA3 was immunoprecipitated from the surrounding medium from the same number of rested and treated platelets (25*10^6/500µl).

4.3. PDIA3 expression is altered in the limbic brain regions of triple-transgenic mouse model of Alzheimer's disease

4.3.1. Alteration of PDIA3 expression in the limbic brain region

PDIA3 protein levels were detected by dot blot assay in all considered cerebral areas. All the obtained data are reported in Figure 20.

In order to evaluate the impact of aging on PDIA3 expression, different brain regions of the limbic system were evaluated in adult and aged Non-Tg mice. We observed a significantly decreased of PDIA3 levels in the amygdala (− 38%, $p < 0.05$) and ventral hippocampus (− 40%, $p < 0.01$) of 18-month-old Non-Tg mice compared to 6-month-old Non-Tg mice; a trend toward a decrease was observed in the entorhinal cortex (− 14%, n.s.).

To evaluate the effect of mild AD-pathology on the PDIA3 levels, 6-month-old 3×Tg-AD mice were evaluated compared to aged-matched Non-Tg mice. Statistical analysis revealed that PDIA3 expression was significantly reduced in the amygdala (− 55%, $p < 0.01$), entorhinal cortex (− 41%, $p < 0.001$) and ventral hippocampus (− 46%, $p < 0.01$).

Finally, to investigate whether the progression of AD-like pathology may be parallel with an altered expression of PDIA3 over time, we evaluated its levels at the mild and severe stage of the disease. Interestingly, 18-month-old 3×Tg-AD mice showed a significant increase of PDIA3 levels in the amygdala (+ 130%, $p < 0.01$) and entorhinal cortex (+ 38%, $p < 0.05$), whilst

a trend toward an increase was observed in ventral hippocampus (+31%, n.s.) compared to 6-month-old 3×Tg-AD mice.

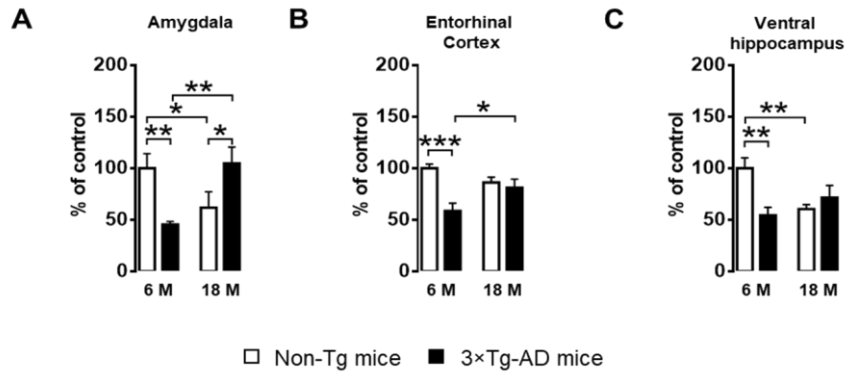

Figure 20. PDIA3 expression levels analyzed by Dot blot.

PDIA3 protein levels were analyzed by Dot-blot in different brain regions of 6- and 18-month-old Non-Tg and 3×Tg-AD mice. Protein levels of all mice were normalized with 6-month-old Non-Tg mice, that was used as control group. All data were analyzed by two-way anova; Tukey's test was used as a post-hoc test to perform multiple comparisons (* $p<0.05$; ** $p<0.01$; *** $p<0.001$). The main brain regions analyzed in this experiment are the following: A: amygdala; B: entorhinal cortex; C: ventral hippocampus.

4.3.2. Aβ/APP-PDIA3 double-fluorescent immunostaining

We performed a double-fluorescent immunostaining on different limbic areas of both 6- and 18-month-old mice, referred as the mild and severe pathology group, respectively. Two of three microphotographs of Aβ/APP-PDIA3 double-fluorescent immunostaining (green and red stain, respectively) and scatterplot analysis of Aβ/APP vs PDIA3 protein levels are shown in Figures 21, 22.

As previously reported [Cassano et al., 2012; Romano et al., 2014; Bellanti et al., 2017], in 3×Tg-AD mice we observed an age-dependent increase of the

Aβ/APP levels in all brain areas investigated in this study. Interestingly, scatterplot analysis indicated a direct correlation between PDIA3 expression and the build-up of Aβ pathology, but with different magnitude among the different brain regions considered. In particular, Pearson correlation test revealed a strong positive correlation in basolateral amygdala ($r = 0.8132$, $p < 0.001$; Fig. 21), whilst a moderate but still positive correlation was observed in entorhinal cortex ($r = 0.6606$, $p < 0.001$; Fig. 22) and in ventral CA1 of hippocampus ($r = 0.3378$, $p < 0.01$; data not shown).

Observing the patterns of PDIA3 subcellular expression, it seems that PDIA3 has increasingly nuclear localization in aged mice of both transgenic and non-transgenic groups which may suggest its possible redistribution during AD development pathology and aging process.

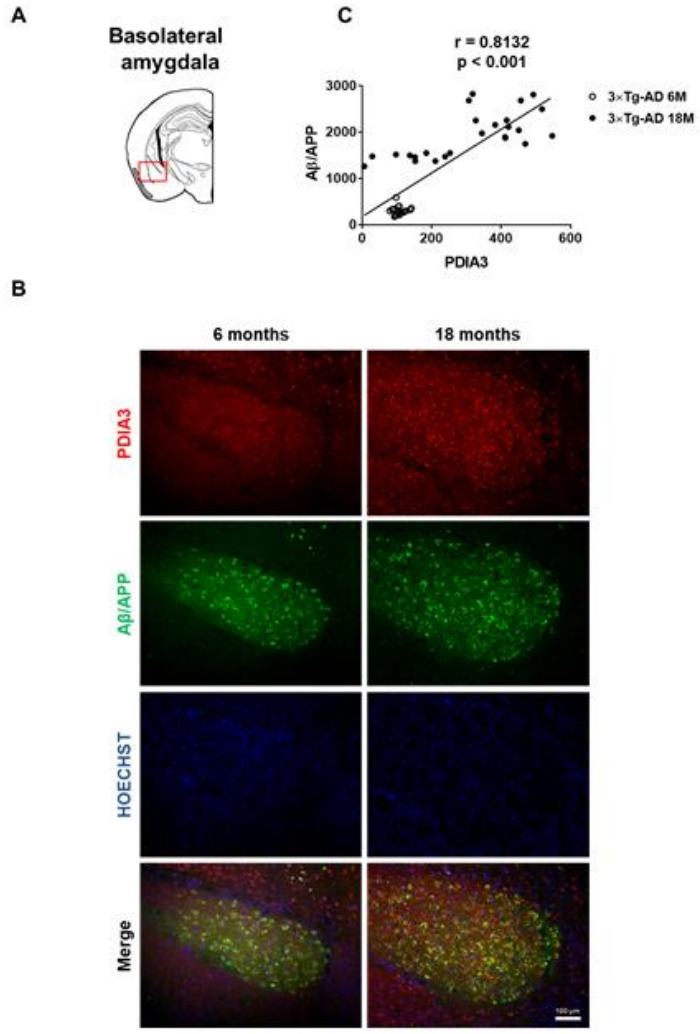

Figure 21. Aβ/APP-PDIA3 double-fluorescent immunostaining. A) Brain diagram which illustrate the site where the representative microphotographs were taken. B) Representative microphotographs of Aβ/APP-PDIA3 double-fluorescent immunostaining (green/red) performed on brain slices collected from 6- and 18-month-old Non-Tg and 3×Tg-AD mice; Hoechst 3342 (blue) was used as fluorescent counterstain. Original magnification: 10×; scale bar was set at 100 μm. C) Scatterplot analyses of Aβ/APP and PDIA3 levels in basolateral amygdala of 3×Tg-AD mice. Aβ/APP and PDIA3 levels were analyzed by Pearson's and normalized with 6-month-old Non-Tg mice, that were used as control group. All data were analyzed by Two Way ANOVA; Tukey's test was used as a post-hoc test to perform multiple comparisons.

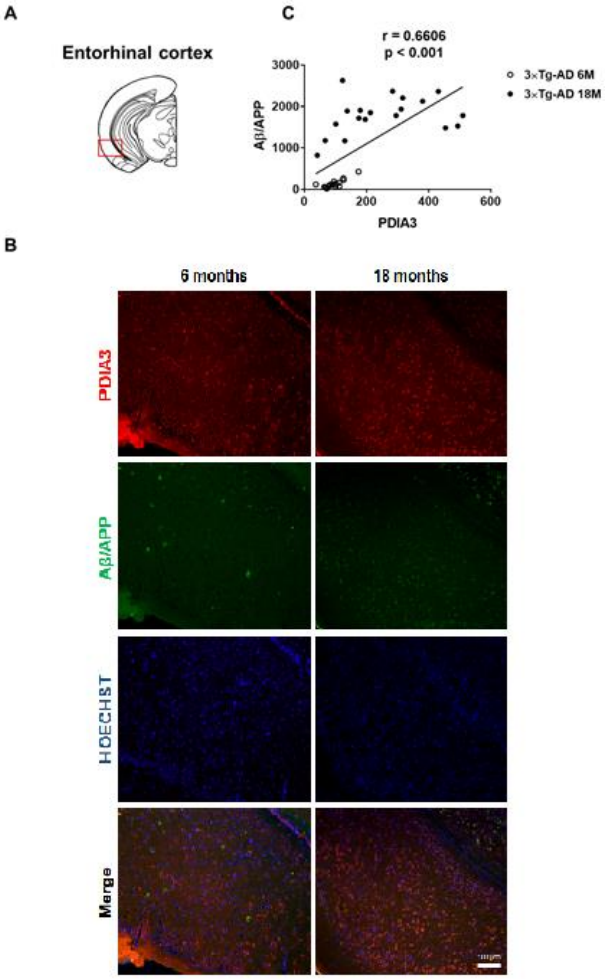

Figure 22. Aβ/APP-PDIA3 double-fluorescent immunostaining. A) Brain diagram which illustrate the site where the representative microphotographs were taken. B) Representative microphotographs of Aβ/APP-PDIA3 double-fluorescent immunostaining (green/red) performed on brain slices collected from 6- and 18-month-old Non-Tg and 3×Tg-AD mice; Hoechst 3342 (blue) was used as fluorescent counterstain. Original magnification: 10×; scale bar was set at 100 μm. C) Scatterplot analyses of Aβ/APP and PDIA3 levels in entorhinal cortex of 3×Tg-AD mice. Aβ/APP and PDIA3 levels were analyzed by Pearson's and normalized with 6-month-old Non-Tg mice, that were used as control group. All data were analyzed by Two Way ANOVA; Tukey's test was used as a post-hoc test to perform multiple comparisons.

4.3.3. GFAP/NeuN/PDIA3 triple-fluorescent immunostaining

Previous studies have reported that PDIA3 transcript is abundantly expressed in all cerebral cell types [Landel et al., 2018], therefore we profiled the pattern of PDIA3 expression in both NeuN-positive differentiated neurons and GFAP-positive astrocytes in both 6- and 18-month-old 3×Tg-AD mice, referred as the mild and severe AD-pathology group, respectively. In particular, a co-immunofluorescence analysis (GFAP-positive astrocytes: blue; NeuN-positive differentiated neurons: green; PDIA3-positive cells: red) was performed in different limbic areas from 3×Tg-AD and age-matched Non-Tg mice. We demonstrated that PDIA3 (red) co-localized with NeuN-positive differentiated neurons (green) in brain regions of both genotypes at both time points considered as reported in two of three representative Figures, 23 and 24. Likewise, PDIA3 (red) co-localized with GFAP-positive astrocytes (blue), whose expression increased with an age-and genotype-dependent fashion in the 3×Tg-AD mice as reported in two of four representative Figures 23 and 24.

Interestingly, we also observed PDIA3-positive staining in several GFAP-positive cells but NeuN-negative cells from all limbic areas (Figures 23 and 24). Therefore, in order to determine to which cell population may belong these PDIA3-positive staining, the signal was detected either in the NeuN channel or in the GFAP channel. Based on the morphology and dimension of PDIA3- positive cells, we hypothesized that these cells may refer to either microglial cells or immature/suffering neurons. To this regard, it has been previously demonstrated that NeuN staining can be altered or lost in immature and/or suffering neurons [Lavezzi et al., 2013].

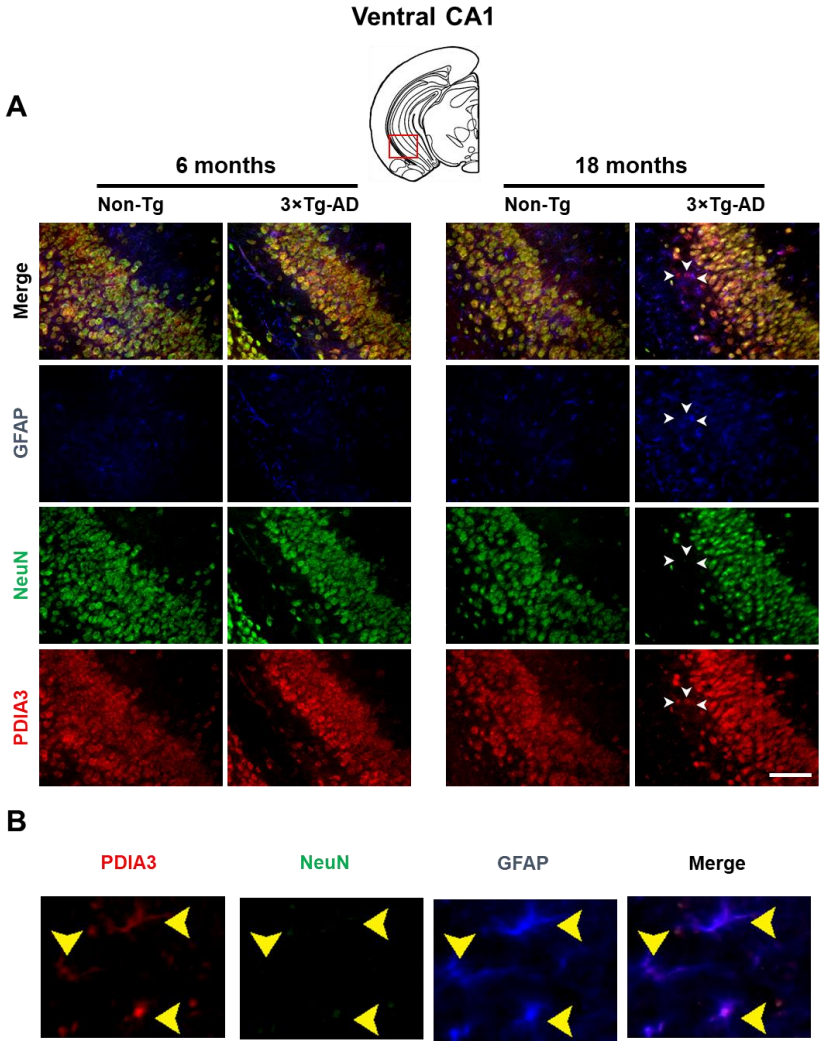

Figure 23. GFAP/NeuN/PDIA3 triple-fluorescent immunostaining.

A) Representative microphotographs of PDIA3/NeuN/GFAP triple-fluorescent immunostaining (red/green/blue) performed on brain slices collected from ventral hippocampus of 6- and 18-month-old Non-Tg and 3×Tg-AD mice. The yellow arrows indicate the PDIA3/GFAP co-localization. Original magnification: 20×; scale bar was set at 100 µm. B) Representative microphotographs of PDIA3/GFAP co-localization in astrocytes of ventral CA1 from 18-month-old 3xTg-AD mice.

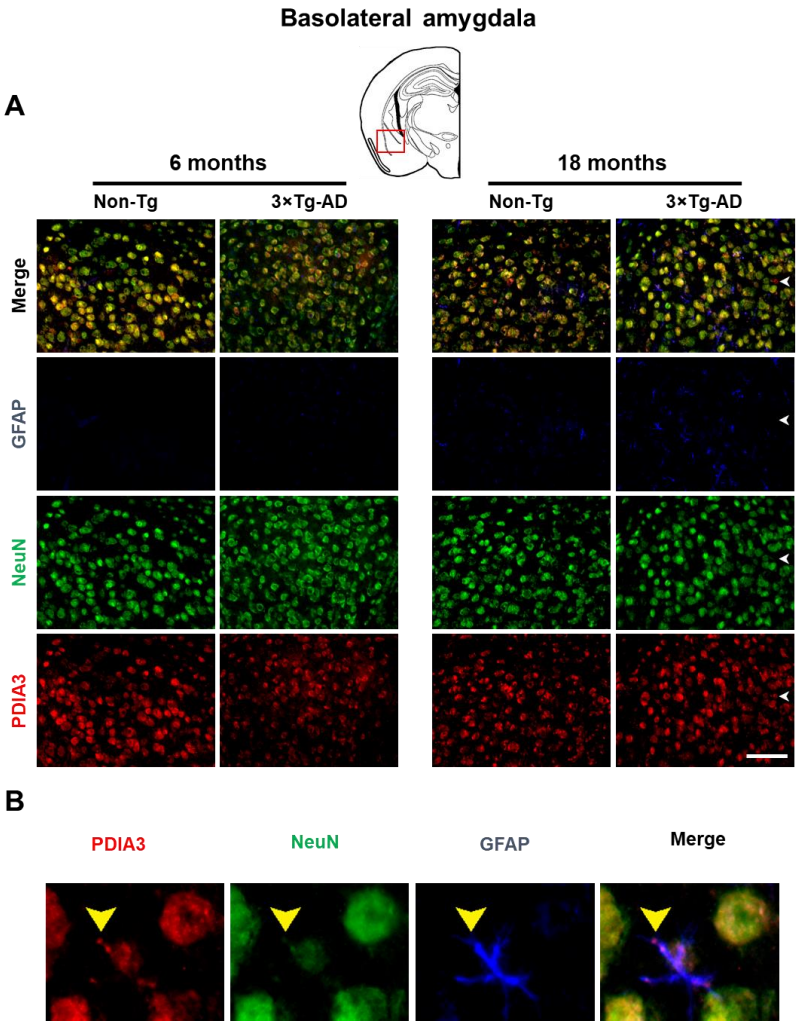

Figure 24. GFAP/NeuN/PDIA3 triple-fluorescent immunostaining.

A) Representative microphotographs of PDIA3/NeuN/GFAP triple-fluorescent immunostaining (red/green/blue) performed on brain slices collected from basolateral amygdala of 6- and 18-month-old Non-Tg and 3×Tg-AD mice. The yellow arrows indicate the PDIA3/GFAP co-localization. Original magnification: 20×; scale bar was set at 100 µm. B) Representative microphotographs of PDIA3/GFAP co-localization in astrocytes of ventral CA1 from 18-month-old 3xTg-AD mice.

Chapter 5: Discussions

5.1. Identification of specific natural PDIA3 interactors able to bind and modulate its activity

The interaction of different natural compounds with PDIA3 and their effect on protein reductase activity were evaluated in a comparative analysis of protein intrinsic fluorescence quenching.

Obtained data revealed a good interaction between PDIA3 and punicalagin, with a K_d in the micromolar range; moreover, its effect on protein fluorescence quenching is consistent with an interaction that involves one or both redox active sites. We also provide evidence that only punicalagin is able to strongly inhibit PDIA3 redox activity and kinetic studies suggest that this compound mainly acts as a non-competitive inhibitor with an estimated K_i of 0.39×10^{-6} M. The binding of punicalagin to PDIA3 was further confirmed by calorimetric titration. Besides, comparative experiments conducted on wild type and PDIA3-silenced neuroblastoma cells suggest the potential of punicalagin to modulate PDIA3 reductase activity also in a biological model. In this regard, we can speculate that punicalagin could be used as a new PDIA3 inhibitor.

Important biological actions have been ascribed to pomegranate, including cardiovascular protection [Aviram et al., 2002]. It was reported that pomegranate juice improves the lipid profiles in diabetic patients with hyperlipidaemia [Esmaillzadeh et al., 2004], while pomegranate flower extract diminishes cardiac fibrosis and improves cardiac lipid metabolism in diabetic rat models [Huang et al., 2005; Huang et al., 2005]. However, the contributions of punicalagin in pomegranate associated cardio-protective benefits remain largely unknown. Conversely, PDIA3 is significantly upregulated in both animal and human models of right and left heart failure and it has been proposed that PDIA3 may regulate SERCA (sarco/endoplasmic reticulum Ca^{2+}-transport ATPase) activity and by extensive contribute to the calcium dysregulation that characterizes progressive heart failure [Vitello et al., 2012]. Then, considering our results, we can hypothesize that some of the cardio-protective effects of punicalagin could be related to its inhibitory activity towards PDIA3.

Considering the different roles played by PDIA3 and its involvement in several types of diseases, finding strong and specific inhibitors of this protein could open a new field in the modulation of its activity and this study represents a starting point in this direction.

5.2. Assessment of PDIA3 involvement in platelet aggregation

Obtained data show that AA and ADP can modulate PDIA3 protein levels in a concentration dependent manner since there was a significant reduction only at 375 µM and 5 µM, respectively (Fig. 18 A-B). Besides, PDIA3 protein levels did not change during platelet aggregation inhibition due to 1

mM PGE1 stimulation (Fig. 17) even if, also in this case, a not significant decrease has been reported. Considering the ability of other PDIs and PDIA3 to be secreted under different platelet aggregation stimuli [Holbrook et al., 2010], the PDIA3 release was also assessed by immunoprecipitation from the surrounding medium of aggregated platelets with AA and ADP and reported data show that PDIA3 can be released also under these stimuli (Fig. 19). In conclusion, considering these observations and previous published data, it can be speculated that PDIA3 is involved in platelet aggregation not via selective pathways. Indeed, not only after thrombin and collagen platelet aggregation induction, but also after AA and ADP stimulation, the PDIA3 decreased and was secreted. Then, it can be assumed that PDIA3 is involved in platelet aggregation not through specific and selective intracellular pathway, mediating by specific platelet inducers, but as a final platelet response independently from triggering stimulus. In addition to PDIA3, it has been reported that many thiol isomerases such as ERp5, ERp72 and PDI can be release from the platelet but the underlying mechanism is not clear [Holbrook et al., 2010]. It is likely that a storage pool of thiol isomerases exists within the platelet and they could be implicated in the regulation of platelet function. Since the release of PDIs might not be mediated by specific stimuli, though it could be the final consequence of platelet aggregation induction, these proteins can be considered new potential and intriguing drug targets.

5.3. The study of PDIA3 profile in brain areas of 3xTg Alzheimer murine model

PDIA3 protein levels were detected by dot blot assay in different limbic areas. A significant decrease of PDIA3 levels in the amygdala, entorhinal

cortex and ventral hippocampus of 6-month-old 3×Tg-AD mice compared to aged-matched Non-Tg mice has been observed, demonstrating the effect of mild AD-pathology on PDIA3 (Fig. 20). The PDIA3 levels were also significantly reduced in the amygdala and ventral hippocampus of 18-month-old Non-Tg mice compared to 6-month-old Non-Tg mice. These data confirm the impact of aging on PDIA3 expression in the considered brain regions (Fig. 20). The endoplasmic reticulum (ER) stress response is regarded as an important process in the aetiology of AD [see for review Hashimoto and Saido, 2018]. The accumulation of pathogenic misfolded proteins is considered to be a fundamental mechanism that underlies the induction of ER stress, leading to neuronal cell death [Costa et al., 2012]. In this scenario, a crucial role seems to be played by the mechanisms for promoting the clearance of neurotoxic and/or misfolded proteins, a strategy that may curtail the onset and slow the progression of AD. Abetas peptides are produced during the normal, post-translational processing of amyloid precursor protein (APP) [Lendon et al., 1997; Pirttila et al. 1994; Selkoe 1999]. Under pathological conditions free abetas readily aggregate to form the insoluble deposits which are a major component of the plaque seen in Alzheimer disease [Pirttila et al. 1994]. Their low solubility suggests that plaque forms when the free, extracellular, abeta concentrations exceed their solubility constants [Lendon et al., 1997; Pirttila et al. 1994; Selkoe 1999]. A group of proteins which may serve as carriers to keep the abetas in solution are the ER chaperones. These have been shown to form complexes with several secretory and plasma membrane proteins [Holtzman 1998]. In this regards, Erickson and colleagues found that the bulk of the abetas were bound to PDIA3 and calreticulin into the cerebrospinal fluid (CSF) of

normals individuals, suggesting that these might be carrier proteins which prevent aggregation of the abetas and that the deposits are due to faulty ER post-translational processing of APP with the failure to form this complex [Erickson et al., 2005]. Our data showed that the intracellular PDIA3 protein amount reduced during the onset of the AD pathology (6-month-old 3×Tg-AD mice) and in condition of aging (18-month-old Non-Tg). Therefore, this can be a consequence of protein secretion, in the view of previous published data, but also protein degradation. Indeed, we excluded the down-regulation of PDIA3 transcription since not relevant changes have been reported by RT-PCR of the considered limbic areas (data not show). Furthermore, many authors have reported the PDIA3 ability to be released in different biological systems [Dihazi et al., 2013; Holbrook et al. 2010; Nardo et al., 2011], in line with the results from Erickson and colleagues, supporting our hypothesis about the possible PDIA3 secretion also in the neuronal system. It is well-established the PDIA3 release from platelets under aggregation condition [Holbrook et al. 2010] or from endothelial cells under vascular injury [Holbrook et al., 2012]. Besides, it has been demonstrated that the secretion of PDIA3 is important for extracellular matrix accumulation and progression of renal fibrosis and is an early sign of disease onset [Dihazi et al., 2013]. Extracellular matrix proteins are translocated into the ER where folding takes place before secretion through the Golgi complex (Bedard et al., 2005; Hebert and Molinari, 2007). Hence, the levels of the chaperons are continuously adjusted to cope with stress conditions and to satisfy the needs of the cell (Dobson, 2003; Goldberg, 2003). Similarly, Almeida and colleagues have showed that the acute knockdown of PDIA3 reduced the progranulin (PGRN) secretion, whose mutations are implicated in the pathogenesis of familial frontotemporal lobar degeneration [Almeida et al., 2011]. This finding was consistent with reports that PDIA3 is required for the

proper secretion of several other substrates [Ellgaard et al., 2005]. The role of secreted PDIA3 was also confirmed by Nardo and colleagues, since they identified PDIA3 and PDIA1 as possible biomarkers to monitor disease progression in blood samples from Amyotrophic Lateral Sclerosis cases [Nardo et al., 2011]. Thus, we can speculate that the intracellular PDIA3 reduction in 6-month old 3xTg-AD mice could be due to its secretion to contrast the development of the disease. The same event could also take place in 18-month old Non-Tg mice in response of stressing condition following to neuronal aging. Due to its chaperone activity, the PDIA3 could be involved in detoxification and protection mechanisms required to help cells in reducing Aβ aggregates formation and their damaging activity in disease condition. In the same aforementioned manner for other pathological conditions, the PDIA3 secretion, in complex with Aβ or other protein, could prevent the development of the AD. Besides, to investigate whether the progression of AD-like pathology may be parallel with an altered expression of PDIA3 over time, we evaluated its levels at the mild and severe stage of the disease. Interestingly, 18-month-old 3×Tg-AD mice showed a significant increase of PDIA3 levels in the amygdala and entorhinal cortex, whilst a trend toward an increase was observed in ventral hippocampus compared to 6-month-old 3×Tg-AD mice. These data demonstrate that PDIA3 is influenced by the mild and severe stage of the AD since PDIA3 protein levels change depending on the transgenic mice age. We hypothesize that, in presence of large amounts of Aβ aggregates due to the severe stage of the AD, PDIA3 can be involved in different pathways respect to its functions in the onset and mild stage of the AD. It has been reported that a depletion of PDIA3 reduced the phosphorylation activity of the mTOR-complex1

[Ramírez-Rangel et al., 2011]. This complex is a key component of a nutrient-sensitive signaling pathway and its activity is relevant for brain functions, regulating energy metabolism, synaptic plasticity as well as cognition. A persistent alteration of neuronal mTOR signaling has been linked to age-dependency cognitive decline and the pathogenesis of AD [Sarbassov et al., 2005; Di Domenico et al. 2017]. In effect, several studies demonstrated that Aβ can enhance mTOR signaling while rapamycin, a mTORC1 inhibitor, significantly reduced intracellular Aβ levels [Caccamo et al., 2010; Caccamo et al., 2011; Talboom JS et al., 2015]. Additionally, it has been reported that PDIA3 is necessary to mTORC1 assembly and affects its function in response to the oxidizing agent PAO. The authors suggested that, by interacting with mTORC1, PDIA3 could be part of the redox-sensing mechanism attributed to mTORC1 [Ramírez-Rangel et al., 2011]. Then, the stressing condition, due to the development of the pathology [Justice 2018; Sotiropoulos et al. 2011], may also alter the PDIA3 redox-sensor activity on mTORC1 contributing to its dysfunction. In this view, PDIA3 level could be relevant in mediating mTOR normal functionality, and either increased or decreased amounts will result in mTOR activity alteration cooperating in AD progression. Finally, the triple-fluorescent immunostaining, using GFAP as marker for astrocytes, NeuN as a marker for neurons and PDIA3, has been performed in limbic areas. Interestingly, the data obtained show the PDIA3-positive staining in several GFAP-positive cells but NeuN-negative cells from all limbic areas (Fig. 23 and 24). We can suppose that those cells could be microglial cells and, indeed, they even appeared in 18-month 3xTg-AD mice. This could be due to the presence of neuroinflammation associated to Alzheimer disease. In fact, Aβ secretion is also related to microglia activation that could lead to a chronic inflammation typical of AD [Morales et al., 2014; Yoo et al., 2015]. Moreover, it has been observed that PDIA3 levels resulted

over-expressed in microglial cells stimulated by Aβ, probably to help the folding of newly synthesized glycoproteins in the ER [Yoo et al., 2015]. PDIA3 could perform a different role in microglial cells respect to neuronal cells. Thus, we can speculate that PDIA3 profile in microglial cells and neurons was completely different; in fact, while at least during the first period of AD the neuronal PDIA3 decreases to contrast the Aβ effects, in microglial cells it may enhance in response of increasing neuroinflammation. More deepen studies need to be performed to prove our hypothesis about the involvement of PDIA3 in Alzheimer disease. However, these preliminary data can be certainly considered a starting point in understanding such a mechanism.

Chapter 6: Conclusions

The goal of my PhD project was to provide new information on the PDIA3 protein, a prominent member of the PDIs family, that could be a pharmacological target in different pathological conditions.

I focused on the PDIA3 involvement in Alzheimer disease and platelet aggregation since limited information are provided by the literature for both conditions. Indeed, the data obtained from my research better clarify some aspect of PDIA3 functions in the two aforementioned situations.

It has been shown that PDIA3 can be also released under AA and ADP platelet aggregation, and not only after thrombin and collagen stimulation. Therefore, the outcomes prove that PDIA3 is involved in platelet aggregation not via selective intracellular pathways, mediating by specific platelet inducers, but as a final platelet response independently from triggering stimulus. This aspect could make the PDIA3 a new potential and intriguing drug target in platelet aggregation pathologies.

Conversely, the data from the Alzheimer's research project clearly demonstrate that PDIA3 has dual profile, maybe performing different roles in the mild and severe stage of the AD. Indeed, in the mild stage of the disease, the reduction of PDIA3 protein levels could be associated to a protective cellular mechanism. At the opposite site, in the severe stage of the disease the re-increasing of the PDIA3 protein levels could be related to harmful effects,

modulating pro-aggressive mechanisms. Hence, in the light of what just said, the PDIA3 functions can be differently modulated in Alzheimer's disease. In the mild stage of the AD the use of positive-PDIA3 interactors such as diosgenin could have beneficial properties in delaying the pathology while PDIA3 inhibitors could be used in repressing its harmful activity in the severe stage. At present, no specific PDIA3 interactors are available to negatively modulate its activity; for this reason, I focused part of my research in discovering possible PDIA3 inhibitors. Our data demonstrate that punicalagin is a new PDIA3 inhibitor with a K_d in the micromolar range and the ability to act as a non-competitive inhibitor with an estimated K_i of 0.39×10^{-6} M. In this regard, punicalagin can be used to modulate PDIA3 activity, on the one hand providing useful information about PDIA3 functions in pathological conditions, and on the other hand using the punicalagin beneficial properties.

References

Adams L. S., N. P. Seeram, B. B. Aggarwal, Y. Takada, D. Sand and D. Heber, "Pomegranate juice, total pomegranate ellagitannins, and punicalagin suppress inflammatory cell signaling in colon cancer cells", J Agric Food Chem, vol. 54, no. 3, pp. 980-985, 2006.

Akhtar S., T. Ismail, D. Fraternale and P. Sestili, "Pomegranate peel and peel extracts: chemistry and food features", Food Chem, vol. 174, no. pp. 417-425, 2015.

Alberdi E, Wyssenbach A, Alberdi M, Sánchez-Gómez MV, Cavaliere F, Rodríguez JJ, Verkhratsky A, Matute C. Ca (2+) -dependent endoplasmic reticulum stress correlates with astrogliosis in oligomeric amyloid β-treated astrocytes and in a model of Alzheimer's disease. Aging Cell. 2013 Apr;12(2):292-302.

Almeida Sandra, Lijuan Zhou, Fen-Biao Gao. Progranulin, a Glycoprotein Deficient in Frontotemporal Dementia, Is a Novel Substrate of Several Protein Disulfide Isomerase Family Proteins. PLoS One. 2011; 6(10): e26454.

Altieri F, Maras B, Eufemi M, Ferraro A, Turano C. Purification of a 57kDa nuclear matrix protein associated with thiol:protein-disulfide oxidoreductase and phospholipase C activities. Biochem. Biophys. Res. Commun. 1993, 194: 992-1000.

Alvarez-Suarez J. M., D. Dekanski, S. Risti´c et al., “Strawberry polyphenols attenuate ethanol-induced gastric lesions in rats by activation of antioxidant enzymes and attenuation of MDA increase,” PLoS ONE, vol. 6, no. 10, article e25878, 2011.

Aviram M., L. Dornfeld, M. Kaplan, R. Coleman, D. Gaitini, S. Nitecki, A. Hofman, M. Rosenblat, N. Volkova, D. Presser, J. Attias, T. Hayek and B. Fuhrman, "Pomegranate juice flavonoids inhibit low-density lipoprotein oxidation and cardiovascular diseases: studies in atherosclerotic mice and in humans", Drugs Exp Clin Res, vol. 28, no. 2-3, pp. 49-62, 2002.

Bedard, K., Szabo, E., Michalak, M. and Opas, M. (2005). Cellular functions of endoplasmic reticulum chaperones calreticulin, calnexin, and ERp57. Int. Rev. Cytol. 245, 91-121.

Bellanti F, Iannelli G, Blonda M, Tamborra R, Villani R, Romano A, Calcagnini S, Mazzoccoli G, Vinciguerra M, Gaetani S, Giudetti AM, Vendemiale G, Cassano T, Serviddio G. Alterations of Clock Gene RNA Expression in Brain Regions of a Triple Transgenic Model of Alzheimer's Disease. J Alzheimers Dis. 2017; 59(2):615-631.

Bi S., D. Song,Y.Tian, X. Zhou,Z. Liu, andH. Zhang, "Molecular spectroscopic study on the interaction of tetracyclines with serum albumins," Spectrochimica Acta—Part A: Molecular and Biomolecular Spectroscopy, vol. 61, no. 4, pp. 629–636, 2005.

Boyan BD, Chen J, Schwartz Z. Mechanism of Pdia3-dependent 1α,25-dihydroxy vitamin D3 signaling in musculoskeletal cells. Steroids. 2012, 77(10): 892-6.

Bravo L., "Polyphenols: chemistry, dietary sources,metabolism, and nutritional significance," Nutrition Reviews, vol. 56, no. 11,pp. 317–333, 1998.

Caccamo A, Majumder S, Richardson A, Strong R, Oddo S. "Molecular interplay between mammalian target of rapamycin (mTOR), amyloid-beta, and Tau: effects on cognitive impairments." J Biol Chem. 2010 Apr 23;285(17):13107-20.

Caccamo A, Maldonado MA, Majumder S, Medina DX, Holbein W, Magrí A, Oddo S. "Naturally secreted amyloid-beta increases mammalian target of rapamycin (mTOR) activity via a PRAS40-mediated mechanism." J Biol Chem. 2011 Mar 18;286(11):8924-32.

Carvalho AT, Fernandes PA, Swart M, Van Stralen JN, Bickelhaupt FM, Ramos MJ. Role of the variable active site residues in the function of thioredoxin family oxidoreductases. J Comput Chem. 2009, 30(5): 710-24.

Cassano T, Serviddio G, Gaetani S, Romano A, Dipasquale P, Cianci S, Bellanti F, Laconca L, Romano AD, Padalino I, LaFerla FM, Nicoletti F, Cuomo V, Vendemiale G. Glutamatergic alterations and mitochondrial impairment in a murine model of Alzheimer disease. Neurobiol Aging. 2012; 33(6):1121.e1-12.

Cheng Z, Zhang J, Ballou DP, Williams CH Jr. Reactivity of thioredoxin as a protein thiol-disulfide oxidoreductase. Chem Rev. 2011, 14;111(9): 5768-83.

Chichiarelli S, Ferraro A, Altieri F, Eufemi M, Coppari S, Grillo C, Arcangeli V, Turano C. The stress protein PDIA3/GRP58 binds specific DNA sequences in HeLa cells. J. Cell. Physiol. 2007, 210: 343-351.

Chichiarelli S, Gaucci E, Ferraro A, Grillo C, Altieri F, Cocchiola R, Arcangeli V, Turano C, Eufemi M. Role of PDIA3 in the signaling and transcriptional activity of STAT3 in a melanoma cell line. Archives of biochemistry and biophysics. 2010, 494: 178-183.

Coe H, Jung J, Groenendyk J, Prins D, Michalak M. PDIA3 modulates STAT3 signaling from the lumen of the endoplasmic reticulum. The Journal of biological chemistry. 2010, 285: 6725-6738.

Coppari S, Altieri F, Ferraro A, Chichiarelli S, Eufemi M, Turano C. Nuclear localization and DNA interaction of protein disulfide isomerase PDIA3 in mammalian cells. J Cell Biochem. 2002, 85 (2): 325-333.

Costa RO, Lacor PN, Ferreira IL, Resende R, Auberson YP, Klein WL, Oliveira CR, Rego AC, Pereira CM. Endoplasmic reticulum stress occurs downstream of GluN2B subunit of N-methyl-d-aspartate receptor in mature hippocampal cultures treated with amyloid-β oligomers. Aging Cell. 2012 Oct;11(5):823-33.

Cui Guozhen, Luchen Shan, Lin Guo, Ivan Keung Chu, Guohui Li, Quan Quan, Yun Zhao, Cheong Meng Chong, Zaijun Zhang, Pei Yu, Maggie Pui Man Hoi, Yewei Sun, Yuqiang Wang, Simon MingYuen Lee. Novel anti-thrombotic agent for modulation of protein disulfide isomerase family member ERp57 for prophylactic therapy. Sci Rep. 2015; 5: 10353.

Cummings JL. Alzheimer's disease. N Engl J Med. 2004 Jul 1;351(1):56-67.

Di Domenico F, Barone E, Perluigi M, Butterfield DA. "The Triangle of Death in Alzheimer's Disease Brain: The Aberrant Cross-Talk Among Energy Metabolism, Mammalian Target of Rapamycin Signaling, and Protein Homeostasis Revealed by Redox Proteomics." Antioxid Redox Signal. 2017 Mar 10;26(8):364-387.

Dick TP, Bangia N, Peaper DR, Cresswell P. Disulfide bond isomerization and the assembly of MHC class I-peptide complexes. Immunity. 2002, 16: 87-98.

Dihazi H, Dihazi GH, Bibi A, Eltoweissy M, Mueller CA, Asif AR, Rubel D, Vasko R, Mueller GA. Secretion of ERP57 is important for extracellular matrix accumulation and progression of renal fibrosis, and is an early sign of disease onset. J Cell Sci. 2013 Aug 15;126(Pt 16):3649-63.

Dihazi H, Dihazi GH, Jahn O, Meyer S, Nolte J, Asif AR, Mueller GA, Engel W. Multipotent adult germline stem cells and embryonic stem cells functional

proteomics revealed an important role of eukaryotic initiation factor 5A (Eif5a) in stem cell differentiation. J. Proteome Res. 2011, 10: 1962-1973.

Dobson, C. M. (2003). Protein folding and misfolding. Nature 426, 884-890.

Dong G, Wearsch PA, Peaper DR, Cresswell P, Reinisch KM. Insights into MHC class I peptide loading from the structure of the tapasin-PDIA3 thioloxidoreductase heterodimer. Immunity. 2009, 30: 21-32.

Du X., Y. Li, Y. L. Xia, S. M. Ai, J. Liang, P. Sang, X. L. Ji and S. Q. Liu, "Insights into Protein-Ligand Interactions: Mechanisms, Models, and Methods", Int J Mol Sci, vol. 17, no. 2, pp. 2016.

Ellerman DA, Myles DG, Primakoff P. A role for sperm surface protein disulfide isomerase activity in gamete fusion: evidence for the participation of PDIA3. Dev. Cell. 2006, 10: 831-837.

Ellgaard L, Ruddock LW (2005) The human protein disulphide isomerase family: substrate interactions and functional properties. EMBO Rep 6: 28–32.

Ellgaard, L., Ruddock, L. W. The human protein disulphide isomerase family: substrate interactions and functional properties. EMBO Rep. 2005; 6(1):28-32.

Erickson RR, Dunning LM, Holtzman JL. The effect of aging on the chaperone concentrations in the hepatic, endoplasmic reticulum of male rats: the possible role of protein misfolding due to the loss of chaperones in the decline in physiological function seen with age. J. Gerontol.Biol.Med. 2006, 61A: 435–443.

Erickson RR, Dunning LM, Olson DA, Cohen SJ, Davis AT, Wood WG, Kratzke RA, Holtzman JL.In cerebrospinal fluid ER chaperones PDIA3 and calreticulin bind beta-amyloid. Biochem Biophys Res Commun. 2005, 332: 50–7.

Esmaillzadeh A., F. Tahbaz, I. Gaieni, H. Alavi-Majd and L. Azadbakht, "Concentrated pomegranate juice improves lipid profiles in diabetic patients with hyperlipidemia", J Med Food, vol. 7, no. 3, pp. 305-308, 2004.

Eufemi M, Coppari S, Altieri F, Grillo C, Ferraro A, Turano C. PDIA3 is present in STAT3-DNA complexes. Biochemical and biophysical research communications. 2004, 323: 1306-1312.

Ferrari DM, Söling HD. The protein disulphide-isomerase family: unravelling a string of folds. Biochem J. 1999; 339 (Pt 1):1-10.

Frank DA. Transcription factor STAT3 as a prognostic marker and therapeutic target in cancer. Journal of clinical oncology : official journal of the American Society of Clinical Oncology. 2013, 31: 4560-4561.

Galligan, J. J., & Petersen, D. R. (2012). The human protein disulfide isomerase gene family. Human Genomics 6, 6.

Garbi N, Tanaka S, Momburg F, Hammerling G.J. Impaired assembly of the major histocompatibility complex class I peptide-loading complex in mice deficient in the oxidoreductase PDIA3. Nat. Immunol. 2006. 7: 93-102.

George V. C., V. V. Vijesh, A. I. Dehigaspege et al., "Mechanism of action of flavonoids in prevention of inflammation associated skin cancer," Current Medicinal Chemistry, vol. 23, no. 32, pp. 3697–3716, 2016.

Goldberg, A. L. (2003). Protein degradation and protection against misfolded or damaged proteins. Nature 426, 895-899.

Grillo C, Coppari S, Turano C, Altieri F. The DNA-binding activity of protein disulfide isomerase PDIA3 is associated with the a(') domain. Biochem Biophys Res Commun. 2002, 295(1): 67-73.

Grillo C, D'Ambrosio C, Consalvi V, Chiaraluce R, Scaloni A, Maceroni M, Eufemi M, Altieri F. DNA-binding activity of the PDIA3 C-terminal domain is related to a redox-dependent conformational change. J. Biol. Chem. 2007, 282: 10299-10310.

Grillo, C., D'Ambrosio, C., Scaloni, A., Maceroni, M., Merluzzi, S., Turano, C., et al. (2006). Cooperative activity of Ref-1/APE and ERp57 in reductive activation of transcription factors. Free Radical Biology & Medicine 41, 1113–1123.

Grindel, B. J., Rohe, B., Safford, S. E., Bennett, J. J., & Farach-Carson, M. C. (2011). Tumor necrosis factor-alpha treatment of HepG2 cells mobilizes a cytoplasmic pool of ERp57/1,25D (3)-MARRS to the nucleus. Journal of Cellular Biochemistry 112, 2606–2615.

Halliwell B., "Oxidative stress and neurodegeneration: where are we now?" Journal of Neurochemistry, vol. 97, no. 6, pp. 1634–1658, 2006.

Hashimoto Shoko and Takaomi C. Saido. Critical review: involvement of endoplasmic reticulum stress in the aetiology of Alzheimer's disease. Open Biol. 2018 Apr; 8(4): 180024

Hatahet F, Ruddock LW: Protein disulfide isomerase. a critical evaluation of its function in disulfide bond formation. Antioxid Redox Signal. 2009, 11(11): 2807-50.

Hatahet, F., & Ruddock, L. W. (2009). Protein disulfide isomerase: A critical evaluation of its function in disulfide bond formation. Antioxidants & Redox Signaling 11, 2807–2850.

He, J., Shi, W., Guo, Y., & Chai, Z. (2014). ERp57 modulates mitochondrial calcium uptake through the MCU. FEBS Letters 588, 2087–2094.

Hebert, D. N. and Molinari, M. (2007). In and out of the ER: protein folding, quality control, degradation, and related human diseases. Physiol. Rev. 87, 1377-1408.

Hertog M. G. L., E. J. M. Feskens, D. Kromhout et al., "Dietary antioxidant flavonoids and risk of coronary heart disease: the Zutphen Elderly Study," The Lancet, vol. 342, no. 8878, pp. 1007–1011, 1993.

Hettinghouse A, Liu R, Liu CJ. Multifunctional molecule ERp57: From cancer to neurodegenerative diseases. Pharmacol Ther. 2018 Jan;181:34-48.

Hetz C, Russelakis-Carneiro M, Walchli S, Carboni S, Vial-Knecht E, Maundrell K, Castilla J, Soto C. The disulfide isomerase Grp58 is a protective factor against prion neurotoxicity. J Neurosci 2005, 25: 2793–802.

Hirano N, Shibasaki F, Sakai R, Tanaka T, Nishida J, Yazaki Y, Takenawa T, Hirai H. Molecular cloning of the human glucose-regulated protein PDIA3/GRP58, a thiol-dependent reductase. Identification of its secretory form and inducible expression by the oncogenic transformation. Eur. J. Biochem. 1995, 234: 336-342.

Holbrook LM, Sasikumar P, Stanley RG, Simmonds AD, Bicknell AB, Gibbins JM. The platelet-surface thiol isomerase enzyme PDIA3 modulates platelet function. J Thromb Haemost. 2012, 10(2):278-288.

Holbrook LM, Watkins NA, Simmonds AD, Jones CI, Ouwehand WH, Gibbins JM. Platelets release novel thiol isomerase enzymes which are recruited to the cell surface following activation. Br J Haematol. 2010 Feb;148(4):627-37.

Holmgren A. Thioredoxin. Annu Rev Biochem. 1985, 54: 237-71.

Holmgren A: Thioredoxin structure and mechanism: conformational changes on oxidation of the active-site sulfhydryls to a disulphide. Structure. 1995, 3: 239-243.

Holtzman J.L., The physiological roles of the thiol:protein disulfide oxidoreductases, in: N. Guzman (Ed.), Prolyl-4-hydroxylase Protein Disulfide Isomerase and Other Structurally Related Proteins, Marcel Dekker, New York, 1998, pp. 173–236.

Huang T. H., G. Peng, B. P. Kota, G. Q. Li, J. Yamahara, B. D. Roufogalis and Y. Li, "Pomegranate flower improves cardiac lipid metabolism in a diabetic rat model: role of lowering circulating lipids", Br J Pharmacol, vol. 145, no. 6, pp. 767-774, 2005.

Huang T. H., Q. Yang, M. Harada, G. Q. Li, J. Yamahara, B. D. Roufogalis and Y. Li, "Pomegranate flower extract diminishes cardiac fibrosis in Zucker diabetic fatty rats: modulation of cardiac endothelin-1 and nuclear factor-kappaB pathways", J Cardiovasc Pharmacol, vol. 46, no. 6, pp. 856-862, 2005.

Hui C., X. Qi, Z. Qianyong, P. Xiaoli, Z. Jundong, and M. Mantian, “Flavonoids, flavonoid subclasses and breast cancer risk: a meta-analysis of epidemiologic studies,” PLoS ONE, vol. 8, no. 1, Article IDe54318, 2013.

Jurenka J. S., "Therapeutic applications of pomegranate (Punica granatum L.): a review", Altern Med Rev, vol. 13, no. 2, pp. 128-144, 2008.

Justice J. Nicholas. The relationship between stress and Alzheimer's disease. Neurobiology of Stress Volume 8, February 2018, Pages 127-133

Khanal, R. C., & Nemere, I. (2007). The ERp57/GRp58/1,25D3-MARRS receptor: Multiple functional roles in diverse cell systems. Current Medicinal Chemistry 14, 1087–1093.

Kim-Han JS, O'Malley KL. Cell stress induced by the parkinsonian mimetic, 6-hydroxydopamine, is concurrent with oxidation of the chaperone, PDIA3, and aggresome formation. Antioxid Redox Signal. 2007, 9(12): 2255-64.

Klappa P., L.W. Ruddock,N. J.Darby, and R. B. Freedman, “The b’ domain provides the principal peptide-binding site of protein disulfide isomerase but all domains contribute to binding of misfolded proteins,” The EMBO Journal, vol. 17, no. 4, pp. 927– 935, 1998.

Kozlov G, Maattanen P, Schrag JD, Pollock S, Cygler M, Nagar B, Thomas DY, Gehring K. Crystal structure of the bb' domains of the protein disulfide isomerase PDIA3. Structure. 2006, 14(8):1331-9.

Lakowicz J. R., Principles of Fluorescence Spectroscopy, Springer, Berlin, Germany, 2006.

Landel V, Stephan D, Cui X, Eyles D, Feron F. Differential expression of vitamin D-associated enzymes and receptors in brain cell subtypes. J Steroid Biochem Mol Biol. 2018; 177:129-134.

Lavezzi AM, Corna MF, Matturri L. Neuronal nuclear antigen (NeuN): a useful marker of neuronal immaturity in sudden unexplained perinatal death. J Neurol Sci. 2013; 329(1-2):45-50.

Lecanu L, Rammouz G, McCourty A, Sidahmed EK, Greeson J, Papadopoulos V. Caprospinol reduces amyloid deposits and improves cognitive function in a rat model of Alzheimer's disease. Neuroscience. 2010 Jan 20;165(2):427-35.

Lee, A. S. (1981). The accumulation of three specific proteins related to glucose-regulated proteins in a temperature-sensitive hamster mutant cell line K12. Journal of Cellular Physiology 106, 119–125.

Lendon C.L., F. Ashall, A.M. Goate, Exploring the etiology of Alzheimer disease using molecular genetics, J. Am. Med. Assoc. 277 (1997) 825–831.

Li Y and Camacho P. Ca2+-dependent redox modulation of SERCA 2b by PDIA3. J. Cell Biol. 2004, 164: 35-46.

Lindquist JA, Jensen ON, Mann M, Hämmerling GJ. ER-60, a chaperone with thiol-dependent reductase activity involved in MHC class I assembly. EMBO J.1998, 17: 2186-2195.

Manach C., A. Scalbert, C.Morand, C. R´em´esy, and L. Jim´enez, “Polyphenols: food sources and bioavailability,” American Journalof Clinical Nutrition, vol. 79, no. 5, pp. 727–747, 2004.

Mandel S. A., T. Amit, O. Weinreb, and M. B. H. Youdim, “Understanding the broad-spectrum neuroprotective action profile of green tea polyphenols in aging and neurodegenerative diseases,” Journal of Alzheimer’s Disease, vol. 25, no. 2, pp. 187–208, 2011.

Mandel S.A., T. Amit,O.Weinreb, L. Reznichenko, andM. B.H. Youdim, “Simultaneous manipulation of multiple brain targets by green tea catechins: a potential neuroprotective strategy for Alzheimer and Parkinson diseases,” CNS Neuroscience and Therapeutics, vol. 14, no. 4, pp. 352–365, 2008.

Marimpietri D, Petretto A, Raffaghello L, Pezzolo A, Gagliani C, Tacchetti C, Mauri P, Melioli G, Pistoia V. Proteome profiling of neuroblastoma-derived exosomes reveal the expression of proteins potentially involved in tumor progression. PLoS One. 2013, 8(9): e75054.

Martin JL, Kenna JG, Martin BM, Thomassen D, Reed GF, Pohl LR. Halothane hepatitis patients have serum antibodies that react with protein disulfide isomerase. Hepatology. 1993, 18: 858–63

Masci A., A. Coccia, E. Lendaro, L. Mosca, P. Paolicelli and S. Cesa, "Evaluation of different extraction methods from pomegranate whole fruit or peels and the

antioxidant and antiproliferative activity of the polyphenolic fraction", Food Chem, vol. 202, no. pp. 59-69, 2016.

McNicol A and Israels S J. Platelets and anti-platelet therapy. J Pharmacol Sci. 2003 Dec;93(4):381-96.

Medjakovic S. and A. Jungbauer, "Pomegranate: a fruit that ameliorates metabolic syndrome", Food Funct, vol. 4, no. 1, pp. 19-39, 2013.

Molinari M and Helenius A. Glycoproteins form mixed disulphides with oxidoreductases during folding in living cells. Nature. 1999, 402: 90-93.

Morales Inelia, Leonardo Guzmán-Martínez, Cristóbal Cerda-Troncoso, Gonzalo A. Farías, Ricardo B. Maccioni. Neuroinflammation in the pathogenesis of Alzheimer's disease. A rational framework for the search of novel therapeutic approaches. Front Cell Neurosci. 2014; 8: 112

Moridani M. Y., J. Pourahmad, H. Bui, A. Siraki, and P. J. O'Brien, "Dietary flavonoid iron complexes as cytoprotective superoxide radical scavengers," Free Radical Biology and Medicine, vol. 34, no. 2, pp. 243–253, 2003.

Moskaug J.O., H. Carlsen, M. C.W.Myhrstad, and R. Blomhoff, "Polyphenols and glutathione synthesis regulation," The American Journal of Clinical Nutrition, vol. 81, no. 1, supplement, pp.277S–283S, 2005.

Muhlenkamp CR, Gill SS. A glucose-regulated protein, GRP58, is down-regulated in C57B6 mouse liver after diethylhexyl phthalate exposure. Toxicol Appl Pharmacol. 1998, 148: 101–8.

Nardo Giovanni, Silvia Pozzi, Mauro Pignataro, Eliana Lauranzano, Giorgia Spano, Silvia Garbelli, Stefania Mantovani, Kalliopi Marinou, Laura Papetti, Marta Monteforte, Valter Torri, Luca Paris, Gianfranco Bazzoni, Christian Lunetta, Massimo Corbo, Gabriele Mora, Caterina Bendotti, Valentina Bonetto. Amyotrophic Lateral Sclerosis Multiprotein Biomarkers in Peripheral Blood Mononuclear Cells. PLoS One. 2011; 6(10): e25545.

Nemere I, Farach-Carson MC, Rohe B, Sterling TM, Norman AW, Boyan BD, Safford SE. Ribozyme knockdown functionally links a 1,25(OH)2D3 membrane binding protein (1,25D3-MARRS) and phosphate uptake in intestinal cells. Proc. Natl. Acad. Sci. USA. 2004, 101: 7392-7397.

Nemere I., N. Garbi, G. Hammerling and K. J. Hintze, "Role of the 1,25D3-MARRS receptor in the 1,25(OH)2D3-stimulated uptake of calcium and phosphate in intestinal cells", Steroids, vol. 10, no. 1878-5867 (Electronic), pp. 897-902, 2012.

Ni M. and A. S. Lee, "ER chaperones in mammalian development and human diseases", FEBS Lett, vol. 581, no. 19, pp. 3641-3651, 2007.

Nishitsuji Kazuchika, Takami Tomiyama, Kenichi Ishibashi, Kazuhiro Ito, Rie Teraoka, Mary P. Lambert, William L. Klein, Hiroshi Mori. The E693Δ Mutation in Amyloid Precursor Protein Increases Intracellular Accumulation of Amyloid β Oligomers and Causes Endoplasmic Reticulum Stress-Induced Apoptosis in Cultured Cells. Am J Pathol. 2009 Mar; 174(3): 957–969.

Oddo S, Caccamo A, Shepherd JD, Murphy MP, Golde TE, Kayed R, Metherate R, Mattson MP, Akbari Y, LaFerla FM. Triple-transgenic model of Alzheimer's disease with plaques and tangles: intracellular Abeta and synaptic dysfunction. Neuron. 2003 Jul 31;39(3):409-21.

Ohtani H, Wakui H, Ishino T, Komatsuda A, Miura AB. An isoform of protein disulfide isomerase is expressed in the developing acrosome of spermatids during rat spermiogenesis and is transported into the nucleus of mature spermatids and epididymal spermatozoa. Histochemistry. 1993, 100: 423-429.

Oliver JD, Roderick HL, Llewellyn DH, High S. PDIA3 functions as a subunit of specific complexes formed with the ER lectins calreticulin and calnexin. Mol. Biol. Cell. 1999, 10: 2573-2582.

Oliver JD, van der Wal FJ, Bulleid NJ, High S. Interaction of the thiol-dependent reductase PDIA3 with nascent glycoproteins. Science. 1997, 275: 86-88.

Ozaki, T., Yamashita, T., & Ishiguro, S. (2008). ERp57-associated mitochondrial mucalpain truncates apoptosis-inducing factor. Biochimica et Biophysica Acta 1783, 1955–1963

Perez-Jimenez J., V. Neveu, F. Vos, and A. Scalbert, “Systematic analysis of the content of 502 Polyphenols in 452 foods and beverages: an application of the phenol-explorer database,” Journal of Agricultural and Food Chemistry, vol. 58, no. 8, pp.4959–4969, 2010.

Pirneskoski A., L. W. Ruddock, P. Klappa, R. B. Freedman, K. I. Kivirikko, and P. Koivunen, “Domains b’ and a’ of protein disulfide isomerase fulfill the minimum requirement for function as a subunit of prolyl 4-hydroxylase: the N-terminal domains a and b enhance this function and can be substituted in part by those of ERp57,” The Journal of Biological Chemistry, vol. 276, no. 14, pp. 11287–11293, 2001.

Pirttila T., K.S. Kim, P.D. Mehta, H. Frey, H.M. Wisniewski, Soluble amyloid beta-protein in the cerebrospinal fluid from patients with Alzheimer’s disease, vascular dementia and controls, J. Neurol. Sci. 127 (1994) 90–95.

Plácido AI, Pereira CM, Duarte AI, Candeias E, Correia SC, Santos RX, Carvalho C, Cardoso S, Oliveira CR, Moreira PI. The role of endoplasmic reticulum in amyloid precursor protein processing and trafficking: implications for Alzheimer's disease. Biochim Biophys Acta. 2014 Sep;1842(9):1444-53.

Ramírez-Rangel I, Bracho-Valdés I, Vázquez-Macías A, Carretero-Ortega J, Reyes-Cruz G, Vázquez-Prado J. Regulation of mTORC1complex assembly and signaling by GRp58/PDIA3. Mol. Cell. Biol. 2011, 31: 1657-1671.

Ramírez-Rangel I, Bracho-Valdés I, Vázquez-Macías A, Carretero-Ortega J, Reyes-Cruz G, Vázquez-Prado J. “Regulation of mTORC1 complex assembly and signaling by GRp58/ERp57” Mol Cell Biol. 2011 Apr;31(8):1657-71.

Raturi A. and B. Mutus, "Characterization of redox state and reductase activity of protein disulfide isomerase under different redox environments using a sensitive fluorescent assay", Free radical biology & medicine, vol. 43, no. 1, pp. 62-70, 2007.

Romano A, Pace L, Tempesta B, Lavecchia AM, Macheda T, Bedse G, Petrella A, Cifani C, Serviddio G, Vendemiale G, Gaetani S, Cassano T. Depressive-like behavior is paired to monoaminergic alteration in a murine model of Alzheimer's disease. Int J Neuropsychopharmacol. 2014; 18(4). pii: pyu020.

Romano Adele, Lorenzo Pace, Bianca Tempesta, Angelo Michele Lavecchia, Teresa Macheda, Gaurav Bedse, Antonio Petrella, Carlo Cifani, Gaetano Serviddio, Gianluigi Vendemiale, Silvana Gaetani, Tommaso Cassano. Depressive-Like Behavior Is Paired to Monoaminergic Alteration in a Murine Model of Alzheimer’s Disease. Int J Neuropsychopharmacol. 2015 Feb; 18(4): pyu020.

Russell SJ, Ruddock LW, Salo KE, Oliver JD, Roebuck QP, Llewellyn DH, Roderick HL, Koivunen P, Myllyharju J, High S. The primary substrate binding site in the b' domain of PDIA3 is adapted for endoplasmic reticulum lectin association. J Biol Chem. 2004, 279(18): 18861-9.

Sarbassov DD, Sabatini DM. “Redox regulation of the nutrient-sensitive raptor-mTOR pathway and complex”. J Biol Chem. 2005 Nov 25;280(47):39505-9.

Schulman Sol, Pavan Bendapudi, Anish Sharda, Vivien Chen, Lola Bellido-Martin, Reema Jasuja, Barbara C. Furie, Robert Flaumenhaft, Bruce Furie. Extracellular Thiol Isomerases and Their Role in Thrombus Formation. Antioxid Redox Signal. 2016 Jan 1; 24(1): 1–15.

Sciandra F, Angelucci E, Altieri F, Ricci D, Hübner W, Petrucci TC, Giardina B, Brancaccio A, Bozzi M. Dystroglycan is associated to the disulfide isomerase PDIA3. Exp Cell Res. 2012, 318(19): 2460-9.

Scuderi Caterina, Maria Rosanna Bronzuoli, Roberta Facchinetti, Lorenzo Pace, Luca Ferraro, Kevin Donald Broad, Gaetano Serviddio, Francesco Bellanti, Gianmauro Palombelli, Giulia Carpinelli, Rossella Canese, Silvana Gaetani, Luca Steardo, Jr, Luca Steardo, Tommaso Cassano. Ultramicronized palmitoylethanolamide rescues learning and memory impairments in a triple transgenic mouse model of Alzheimer's disease by exerting anti-inflammatory and neuroprotective effects. Transl Psychiatry. 2018; 8: 32.

Seeram N. P., R. N. Schulman and D. Heber, Pomegranates: Ancient roots to modern medicine, CRC Press,2006.

Sehgal PB. Plasma membrane rafts and chaperones in cytokine/ STAT signaling. Acta Biochim Pol. 2003, 50(3): 583-94.

Seliger B, Wollscheid U, Momburg F, Blankenstein T, Huber C. Characterization of the major histocompatibility complex class I deficiencies in B16 melanoma cells. Cancer Res. 2001, 61: 1095–9.

Selivanova A, Winblad B, Dantuma NP, Farmery MR. Biogenesis and processing of the amyloid precursor protein in the early secretory pathway. Biochem Biophys Res Commun. 2007 Jun 15;357(4):1034-9.

Selkoe D.J., Translating cell biology into therapeutic advances in Alzheimer's disease, Nature 399 (Suppl. 24) (1999) A23–A31

Sepulveda M, Rozas P, Hetz C, Medinas DB. "ERp57 as a novel cellular factor controlling prion protein biosynthesis: Therapeutic potential of protein disulfide isomerases." Prion. 2016;10(1):50-6. doi: 10.1080/19336896.2015.1129485.

Seyb Kathleen I., Sabah Ansar, Jennifer Bean, Mary L. Michaelis. β-amyloid and endoplasmic reticulum stress reponses in primary neurons. J Mol Neurosci (2006) 28: 111.

Silvennoinen, L., Myllyharju, J., Ruoppolo, M., Orru, S., Caterino, M., Kivirikko, K. I., et al. (2004). Identification and characterization of structural domains of human ERp57: Association with calreticulin requires several domains. The Journal of Biological Chemistry 279, 13607–13615.

Song JI, Grandis JR. STAT signaling in head and neck cancer. Oncogene. 2000, 19: 2489-2495

Sotiropoulos Ioannis, Caterina Catania, Lucilia G. Pinto, Rui Silva, G. Elizabeth Pollerberg, Akihiko Takashima, Nuno Sousa and Osborne F. X. Almeida. Stress

Acts Cumulatively To Precipitate Alzheimer's Disease-Like Tau Pathology and Cognitive Deficits. Journal of Neuroscience 25 May 2011, 31 (21) 7840-7847;

Talboom JS, Velazquez R, Oddo S. “The mammalian target of rapamycin at the crossroad between cognitive aging and Alzheimer's disease.” NPJ Aging Mech Dis. 2015 Oct 15;1:15008.

Tohda C, Urano T, Umezaki M, Nemere I, Kuboyama T. Diosgenin is an exogenous activator of 1,25D3-MARRS/Pdia3/PDIA3 and improves Alzheimer’s disease pathologies in 5XFAD mice. Sci Rep. 2012, 2: 535.

Tourkova IL, Shurin GV, Chatta GS, Perez L, Finke J, Whiteside TL, Ferrone S, Shurin MR.. Restoration by IL-15 of MHC class I antigen-processing machinery in human dendritic cells inhibited by tumor-derived gangliosides. J Immunol 2005, 175: 3045–52.

Trnkova L., D. Ricci, C. Grillo, G. Colotti and F. Altieri, "Green tea catechins can bind and modify ERp57/PDIA3 activity", Biochim Biophys Acta, vol. 1830, no. 3, pp. 2671-2682, 2013.

Turano C, Coppari S, Altieri F, Ferraro A. Proteins of the PDI family: unpredicted non-ER locations and functions. J Cell Physiol. 2002, 193(2): 154-63.

Turrini E., L. Ferruzzi and C. Fimognari, "Potential Effects of Pomegranate Polyphenols in Cancer Prevention and Therapy", Oxid Med Cell Longev, vol. 2015, no. pp. 938475, 2015.

Vauzour D., A. Rodriguez-Mateos, G. Corona, M. J. Oruna- Concha, and J. P. E. Spencer, “Polyphenols and human health: prevention of disease andmechanisms of action,” Nutrients, vol.2, no. 11, pp. 1106–1131, 2010.

Vitello A. M., Y. Du, P. M. Buttrick and L. A. Walker, "Serendipitous discovery of a novel protein signaling mechanism in heart failure", Biochem Biophys Res Commun, vol. 421, no. 3, pp. 431-435, 2012.

Wang Lu, Yi Wu, Junsong Zhou, Syed S. Ahmad, Bulent Mutus, Natalio Garbi, Günter Hämmerling, Junling Liu, David W. Essex. Platelet-derived ERp57 mediates platelet incorporation into a growing thrombus by regulation of the αIIbβ3 integrin Blood. 2013 Nov 21; 122(22): 3642–3650.

Williams R. J., J. P. E. Spencer, and C. Rice-Evans, “Flavonoids: antioxidants or signalling molecules?” Free Radical Biology and Medicine, vol. 36, no. 7, pp. 838–849, 2004.

Woo H. D. and J. Kim, “Dietary flavonoid intake and smokingrelated cancer risk: a meta-analysis,” PLoS ONE, vol. 8, no. 9, article e75604, 2013

Wu Y, Ahmad SS, Zhou J, Wang L, Cully MP, Essex DW. The disulfide isomerase PDIA3 mediates platelet aggregation, hemostasis, and thrombosis. Blood. 2012, 119(7):1737-1746.

Wu, W., Beilhartz, G., Roy, Y., Richard, C. L., Curtin, M., Brown, L., et al. (2010). Nuclear translocation of the 1,25D3-MARRS (membrane associated rapid response to steroids) receptor protein and NFkappaB in differentiating NB4 leukemia cells. Experimental Cell Research 316, 1101–1108.

Yoo Y, Byun K, Kang T, Bayarsaikhan D, Kim JY, Oh S, Kim YH, Kim SY, Chung WI, Kim SU, Lee B, Park YM. "Amyloid-beta-activated human microglial cells through ER-resident proteins." J Proteome Res. 2015 Jan 2;14(1):214-23.

Yu H, Jove R. The STATs of cancer-new molecular targets come of age. Nature reviews. Cancer. 2004, 4: 97-105.

Yu H, Pardoll D, Jove R. STATs in cancer inflammation and immunity: a leading role for STAT3. Nature reviews. Cancer. 2009, 9: 798-809.

Zhou Junsong, Yi Wu, Lu Wang, Lubica Rauova, Vincent M. Hayes, Mortimer Poncz, David W. Essex. The disulfide isomerase ERp57 is required for fibrin deposition in vivo. J Thromb Haemost. 2014 Nov; 12(11): 1890–1897.

Ringraziamenti

Il primo doveroso ringraziamento per questo nuovo traguardo raggiunto va sicuramente al mio supervisor, Prof. Fabio Altieri. Vorrei ringraziarlo per essere stato una guida, per essere stato sempre aperto al confronto, per aver sempre ascoltato il mio umile parere, per avermi dato spunti da cui partire e su cui riflettere, per aver avuto la pazienza e la voglia di insegnarmi la maggior parte delle cose che so. Ha saputo sempre sostenermi ed aiutarmi, lasciandomi ogni tanto cadere per poter imparare dai miei errori e per questo vorrei dirle semplicemente “Grazie”.

Subito a seguire vorrei ringraziare la Prof. Margherita Eufemi e la Dott.ssa Silvia Chichiarelli per essermi state sempre vicine, incoraggiandomi, supportandomi e dimostrandomi il loro affetto sia in laboratorio ma anche nella vita di tutti i giorni. Ne approfitto anche per ringraziare il Prof. Francesco Malatesta, coordinatore del dottorato, per tutti i consigli, per le chiacchierate di scienza e soprattutto per la sua immensa pazienza con me.

Un altro doveroso ringraziamento va alla mia famiglia, mia madre e mia sorella. In questi tre anni sono state più che mai la mia ancora, la mia forza, la mia determinazione ma anche le mie più acerrime nemiche. Ad ogni modo questo non ha fatto altro che rafforzare quello che già era duro e resistente come l’acciaio. Più che mai ho capito che quello che abbiamo noi tre

difficilmente si riesce a trovare e per questo le uniche parole che ho da dirvi sono “Grazie” e “Vi voglio bene”.

Il prossimo non può che non essere lui, Andrea Vanzo, il mio compagno da sempre ormai, colui con cui sono cresciuta e che vorrei con me per tutta la vita. Sono stati tempi difficili per noi questi due anni ma, come sempre, siamo riusciti ad essere l’uno la spalla dell’altro. Vorrei dirti grazie per essere stato sempre prima il mio più grande “fans” e poi il mio compagno.

Adesso loro, le mie amiche Lale, Ge, Marta e Gi. A voi che siete le mie sorelle va il ringraziamento di esserci sempre state, di aver fatto cose matte per me (vedi Hradec Kralove), per avermi dato i miei bellissimi nipoti Ale e Gabri, per le risate, i pianti e le gioie. Inoltre, insieme a voi ne approfitto per ringraziare tutto il mio gruppo del “paese”, cosi non sono costretta a dover fare l’elenco dei nomi che sarebbe infinito, per il calore che siete riusciti a darmi in questi ultimi anni, siete stupendi.

Nella lista degli amici non posso che ringraziare tutti i miei amici del Dip. “A. Rossi Fanelli” partendo dal mio lab 204-232, passando per il piano terra ed arrivando nel mio piano “adottivo”, il -1. Anche qui la lista dei nomi sarebbe infinita considerando tutte le persone che ho conosciuto in questi tre anni e che oggi porto nel cuore più che mai. Grazie delle belle giornate passate, delle cene alle 10 di sera in laboratorio, delle risate, dei roof beer, delle chiacchiere, semplicemente grazie di tutto. Uno speciale ringraziamento va però alle Dottoresse Lisa Beatrice Caruso e Ilaria Marrocco. Con voi è nata “Poppy”, la ragazzina del ’90 che poi più tanto piccola non è. Grazie per essere state le mie insegnati e le mie supporters ma soprattutto le mie amiche.

Un altro ringraziamento dal cuore va alla famiglia del mio compagno. Grazie per essere stati una famiglia per me quando mi sentivo sola e per

avermi sempre aiutato in tutto. Un piccolo ma grande Grazie è tutto per i miei nipoti Matteo e Martina per riuscire sempre a strapparmi un sorriso.

Last but not least, vorrei ringraziare tutti i ragazzi de “La Via del Sale Onlus”. Il terremoto ha spezzato vite, ha spezzato legami ma ha altrettanto creato nuovi legami, di amicizia e di amore. Sono felice di far parte di questa immensa famiglia. A voi vorrei dire grazie per avermi fatto sentirsi utile per qualcuno. Vedere da vicino la disperazione delle persone e sapere di poter contribuire ad aiutarle mi ha permesso di allietare un po’ il mio dolore. Mi ha fatto capire che tutto il male del mondo non può distruggere la determinazione delle persone e tante volte è stato per me la spinta a cui mi sono aggrappata.

Vorrei concludere questi miei ringraziamenti dedicando questo mio elaborato e quindi questo percorso di vita a mio padre. Ho deciso di dedicarglielo perché, anche se non avrebbe capito una parola di quello che c’è scritto e avrei dovuto impiegare forse due mesi per fargli capire cosa era il dottorato e in cosa mi ero dottorata, so che lui sarebbe stato fiero di me. Avrebbe avuto gli occhi lucidi alla proclamazione e avrebbe offerto da bere anche alle statue della Sapienza durante i festeggiamenti. Una lacrima scende ma lo so che da qualche parte chissà potrai vedermi e sentirmi e io riuscirò a percepire il tuo orgoglio.

Chapter 7: Appendix

The Appendix collects the front page of my publications.

Hindawi Publishing Corporation
Oxidative Medicine and Cellular Longevity
Volume 2016, Article ID 4518281, 12 pages
http://dx.doi.org/10.1155/2016/4518281

Research Article

Comparative Analysis of the Interaction between Different Flavonoids and PDIA3

Flavia Giamogante,[1] Ilaria Marrocco,[1] Donatella Romaniello,[1] Margherita Eufemi,[1,2] Silvia Chichiarelli,[1,2] and Fabio Altieri[1,2]

[1]*Department of Biochemical Sciences "A. Rossi Fanelli", Sapienza University, P.le A. Moro 5, 00185 Rome, Italy*
[2]*Istituto Pasteur-Fondazione Cenci Bolognetti, Sapienza University, P.le A. Moro 5, 00185 Rome, Italy*

Correspondence should be addressed to Fabio Altieri; fabio.altieri@uniroma1.it

Received 23 September 2016; Accepted 6 November 2016

Academic Editor: Thea Magrone

Flavonoids, plant secondary metabolites present in fruits, vegetables, and products such as tea and red wine, show antioxidant, anti-inflammatory, antithrombotic, antiviral, and antitumor activity. PDIA3 is a member of the protein disulfide isomerase family mainly involved in the correct folding of newly synthetized glycoproteins. PDIA3 is associated with different human pathologies such as cancer, prion disorders, Alzheimer's disease, and Parkinson's diseases and it has the potential to be a pharmacological target. The interaction of different flavonoids with PDIA3 was investigated by quenching fluorescence analysis and the effects on protein activity were evaluated. A higher affinity was observed for eupatorin-5-methyl ether and eupatorin which also inhibit reductase activity of PDIA3 but do not significantly affect its DNA binding activity. The use of several flavonoids differing in chemical structure and functional groups allows us to make some consideration about the relationship between ligand structure and the affinity for PDIA3. The specific flavone backbone conformation and the degree of polarity seem to play an important role for the interaction with PDIA3. The binding site is probably similar but not equivalent to that of green tea catechins, which, as previously demonstrated, can bind to PDIA3 and prevent its interaction with DNA.

1. Introduction

PDIA3/ERp57 is a member of the protein disulfide isomerase family mainly present in the endoplasmic reticulum, where it carries out a major role as a key molecular player in the quality control and correct folding of newly synthesized glycoproteins [1]. However, PDIA3 has been found in different subcellular compartments where it has been proposed and sometimes proved to be involved in a remarkable variety of cellular processes and in pathological conditions including cancer and neurodegenerative diseases. This is documented by the evergrowing number of published results summarized in some recent reviews [2–4].

The specific enzymatic activity and wide binding capabilities of PDIA3 may allow its interaction with many other proteins. PDIA3 has been thought to be a participant in the mechanisms of cell protection against oxidative stress through its redox and chaperone activities but target substrates remain to be ascertained. Many studies suggest that PDIA3 can prevent oxidation of thiol residues and aggregation of target proteins which might result in a loss of functional and/or structural properties [5–7]. Expression of PDIA3 is increased in more than 70% of cancers and its expression has been associated with cell invasiveness, metastasis, and low overall survival. PDIA3 may play a role in the oncogenic transformation as a result of its ability to control intracellular and extracellular redox state via thiol-dependent reductase activity [8, 9]. Moreover, PDIA3 may be engaged in cellular signalling pathways involving reactive oxygen species: it may rescue the functional activity of target proteins that undergo redox modification and/or control the formation of macromolecular complexes involved in the adaptive response to oxidative stress.

In this contest, the identification of specific substances able to bind PDIA3 and to modify its properties will be very useful. Considering the high level of PDIA3 expression in several cancer types, specific inhibitors might offer new

Biochimie 147 (2018) 122–129

Contents lists available at ScienceDirect

Biochimie

journal homepage: www.elsevier.com/locate/biochi

Research paper

Punicalagin, an active pomegranate component, is a new inhibitor of PDIA3 reductase activity

Flavia Giamogante, Ilaria Marrocco [1], Laura Cervoni, Margherita Eufemi, Silvia Chichiarelli, Fabio Altieri*

Department of Biochemical Sciences, "A. Rossi Fanelli" and Istituto Pasteur-Fondazione Cenci Bolognetti, Sapienza University, P.le A. Moro 5, 00185, Rome, Italy

ARTICLE INFO

Article history:
Received 15 November 2017
Accepted 31 January 2018
Available online 6 February 2018

Keywords:
Punicalagin
Pomegranate extracts
PDIA3/ERp57
Ligand-protein binding
Oxidative stress
PDIA3 inhibitor

ABSTRACT

Background: Polyphenolic compounds isolated from pomegranate fruit possess several pharmacological activities including anti-inflammatory, hepatoprotective, antigenotoxic and anticoagulant activities. The present work focuses the attention on PDIA3 interaction with punicalagin and ellagic acid, the most predominant components of pomegranate extracts. PDIA3, a member of the protein disulfide isomerase family involved in several cellular functions, is associated with different human diseases and it has the potential to be a pharmacological target.
Methods: The interaction of polyphenols with PDIA3 purified protein was explored by fluorescence quenching and calorimetric techniques and their effect on PDIA3 activity was investigated.
Results: A higher affinity was observed for punicalagin which also strongly affects PDIA3 reductase activity *in vitro* as a non-competitive inhibitor. Isothermal titration calorimetry confirmed the high affinity of punicalagin for PDIA3. Considering the PDIA3 involvement in oxidative cellular stress response observed in neuroblastoma cells after treatment with hydrogen peroxide, a comparative study was conducted to evaluate the effect of punicalagin on wild type and PDIA3-silenced cells. Punicalagin increases the cell sensitivity to hydrogen peroxide in neuroblastoma cells, but this effect is drastically reduced in PDIA3-silenced cells treated in the same experimental conditions.
Conclusions: Punicalagin binds PDIA3 and inhibits its redox activity. Comparative experiments conducted on unsilenced and PDIA3-silenced neuroblastoma cells suggest the potential of punicalagin to modulate PDIA3 reductase activity also in a biological model.
General significance: Punicalagin can be used as a new PDIA3 inhibitor and this can provide information on the molecular mechanisms underlying the biological activities of PDIA3 and punicalagin.

1. Introduction

Protein disulfide isomerase isoform A3 (PDIA3), also known as ERp57, GRP58 and 1,25-D3-MARRS, is a member of the protein disulfide isomerase family; it is a protein of 505 aminoacids and molecular weight of 57 kDa with a structure characterized by four tioredoxin-like domains: *a*, *b*, *b*' and *a*'. The *a* and *a*' domains contain the catalytic active sites constituted by the tetrapeptide CGHC, which provides PDIA3 with redox activity, while *b* and *b*' domains are redox inactive but are required for the PDIA3 complete activity [1–3]. PDIA3 is localized predominantly in the endoplasmic reticulum, where it is involved in the correct folding of newly synthetized glycoproteins and in the assembly of the MHC class I complex [4–6]. It is also present in the cytosol where it can interact

Abbreviations: DiE-GSSG, dieosin glutathione disulfide; DTT, dithiothreitol; EDTA, ethylenediaminetetraacetic acid; GSSG, oxidized glutathione; HEPES, 4-(2-hydroxyethyl)-1-piperazineethanesulfonic acid; PDIA3, protein disulfide isomerase isoform A3; PBS, phosphate buffered saline; TCEP, tris(2-carboxyethyl) phosphine; DMSO, dimethyl sulfoxide; FBS, fetal bovine serum; XTT, sodium 3'- [1-(phenylaminocarbonyl)- 3,4- tetrazolium]-bis (4-methoxy- 6-nitro) benzene sulfonic acid hydrate.

* Corresponding author. Department of Biochemical Sciences, "A. Rossi Fanelli" and Istituto Pasteur – Fondazione Cenci Bolognetti, Sapienza University, P. le A. Moro 5, IT-00185, Rome, Italy.
E-mail address: fabio.altieri@uniroma1.it (F. Altieri).
[1] Present address: Department of Biological Regulation, Weizmann Institute of Science, 234 Herzl Street Rehovot, 7610001 Israel.

https://doi.org/10.1016/j.biochi.2018.01.008
0300-9084/

International Journal of
Molecular Sciences

MDPI

Article

STAT3, a Hub Protein of Cellular Signaling Pathways, Is Triggered by β-Hexaclorocyclohexane

Elisabetta Rubini [1], Fabio Altieri [1,2], Silvia Chichiarelli [1], Flavia Giamogante [1], Stefania Carissimi [1], Giuliano Paglia [1], Alberto Macone [1] and Margherita Eufemi [1,2,*]

[1] Department of Biochemical Sciences, A. Rossi Fanelli, Sapienza University, P.le A. Moro 5, 00185 Rome, Italy; elisabetta.rubini@uniroma1.it (E.R.); fabio.altieri@uniroma1.it (F.A.); silvia.chichiarelli@uniroma1.it (S.C.); flavia.giamogante@uniroma1.it (F.G.); stefania.carissimi@uniroma1.it (S.C.); giuliano.pag@gmail.com (G.P.); alberto.macone@uniroma1.it (A.M.)

[2] Istituto Pasteur-Fondazione Cenci Bolognetti, Sapienza University, P.le A. Moro 5, 00185 Rome, Italy

* Correspondence: margherita.eufemi@uniroma1.it; Tel.: +39-06-49910598

Received: 26 June 2018; Accepted: 17 July 2018; Published: 20 July 2018

Abstract: Background: Organochlorine pesticides (OCPs) are widely distributed in the environment and their toxicity is mostly associated with the molecular mechanisms of endocrine disruption. Among OCPs, particular attention was focused on the effects of β-hexaclorocyclohexane (β-HCH), a widely common pollutant. A detailed epidemiological study carried out on exposed population in the "Valle del Sacco" found correlations between the incidence of a wide range of diseases and the occurrence of β-HCH contamination. Taking into account the pleiotropic role of the protein signal transducer and activator of transcription 3 (STAT3), its function as a hub protein in cellular signaling pathways triggered by β-HCH was investigated in different cell lines corresponding to tissues that are especially vulnerable to damage by environmental pollutants. Materials and Methods: Human prostate cancer (LNCaP), human breast cancer (MCF-7 and MDA-MB 468), and human hepatoma (HepG2) cell lines were treated with 10 μM β-HCH in the presence or absence of specific inhibitors for different receptors. All samples were subjected to analysis by immunoblotting and RT-qPCR. Results and Conclusions: The preliminary results allow us to hypothesize the involvement of STAT3, through both its canonical and non-canonical pathways, in response to β-HCH. Moreover, we ascertained the role of STAT3 as a master regulator of energy metabolism via the altered expression and localization of HIF-1α and PKM2, respectively, resulting in a Warburg-like effect.

Keywords: STAT3; β-hexaclorocyclohexane (β-HCH); signal transduction; energy metabolism

1. Introduction

Organochlorine compounds are widely distributed in the environment and several studies link their basic molecular mechanism of endocrine disruption [1,2] with the onset of many pathological conditions such as chronic inflammatory processes, cardiovascular diseases, neurological and metabolic disorders, and oncogenesis [3–5]. The toxicity of organochlorine compounds is related to their physicochemical properties, because these pollutants belong to a group of organic compounds, known as "persistent organic pollutants" (POPs), that are resistant to degradation or biodegradation and that can be bioaccumulated into adipose tissue because of their lipotropic properties and great stability [6]. Observational epidemiological studies, carried out on population at high risk of exposure, revealed that POPs may play an important role in the development of a chronic inflammatory state by interfering with pathways associated with essential cellular processes and homeostasis [7]. Acute inflammation represents one of the early responses to injury but, if the causal insult becomes persistent, it may progress with a long chronic phase; although acute inflammation is necessary to rid the organism of